

---

# RECONSTRUCTING FHDE WITH SCALAR AND GAUGE FIELDS

---

A PREPRINT

 **Ayush Bidlan**\*

*Department of Physics,  
Sardar Vallabhbhai National Institute of Technology,  
Surat 395007, Gujarat, India*

 **Paulo Moniz**†

*Departamento de Física, Centro de Matemática e Aplicações (CMA-UBI),  
Universidade da Beira Interior,  
Marquês d'Avila e Bolama, 6200-001 Covilhã, Portugal*

 **Oem Trivedi**‡

*International Centre for Space and Cosmology,  
Ahmedabad University,  
Ahmedabad 380009, India*

February 4, 2025

## ABSTRACT

We revisit the Fractional Holographic Dark Energy (FHDE) model to reconstruct it by means of dynamic candidates such as (i) Quintessence, (ii) K-essence, (iii) Dilaton, (iv) Yang-Mills condensate, (v) DBI-essence, and (vi) Tachyonic fields in a flat Friedmann-Robertson-Walker (FRW) Universe. In particular, the dark-energy possibilities (i)-(vi) are formulated through suitable field descriptions. Being concrete, we establish a comprehensive correspondence between FHDE and suitable scalar and gauge field frameworks that co-substantiate our investigation and subsequent discussion. In more detail, we methodically compute the corresponding Equation of State (EoS) parameters and field (kinetic and potential) features for the fractional parameter ( $\alpha$ ) range, viz.  $1 < \alpha \leq 2$ . Conclusively, our results show that the modifications brought by the fractional features satisfactorily enable late-time cosmic acceleration, together with avoiding quantum instabilities by preventing the EoS from entering the phantom divide i.e.,  $\omega(z) \rightarrow -\infty$ , which is a common issue in standard scalar field models without fractional dynamics (e.g., K-essence field). Our findings further indicate that fractional calculus attributes can be significant in addressing the challenges of dark-energy models by offering a robust framework to prospect late-time acceleration and properly fitting observational constraints. Notably, we find that as the fractional features start to dominate, the EoS parameter of all the effective field configurations asymptotically approaches a  $\Lambda$ CDM behaviour in the far-future limit  $z \rightarrow -1$ . In summary, the recent perspective introduced by FHDE [Trivedi et al., 2024] can indeed be cast as a promising aspirant through the use of prominent field frameworks.

**Keywords** Holographic Principle · Dynamic Dark Energy · Fractional Quantum Cosmology

## 1 Introduction

The mysterious nature of dark energy has been teasing us, constituting so far an obstacle blocking our understanding of the Universe ever since its observational inception in the late twentieth century [Riess et al., 1998, Perlmutter et al.,

---

\*:i21ph018@phy.svnit.ac.in

†pmoniz@ubi.pt

‡oem.t@ahduni.edu.in

1999]. Observations of phenomena such as Type Ia Supernovae (SNe Ia) [Astier et al., 2006, Riess et al., 2004, 2007, Wood-Vasey et al., 2007, Davis et al., 2007, Kowalski et al., 2008], the Cosmic Microwave Background (CMB) [Spergel et al., 2003, 2007, Komatsu et al., 2009, 2011] and Baryon Acoustic Oscillations (BAOs) [Eisenstein et al., 2005, Percival et al., 2007, 2010] have vindicated the presence of dark energy, estimated to constitute a substantial proportion ( $\sim 70\%$ ) of the Universe. The traditional method for tackling late-time cosmic acceleration has been based on the addition of a cosmological constant, denoted by  $\Lambda$ , to the field equations of the General Theory of Relativity [Weinberg, 1989, Padmanabhan, 2003]. This constant serves as a type of dark energy that permeates space, inducing a peculiar dynamics that opposes e.g. Newtonian attractive gravity, fuelling an accelerated expansion of the Universe. The scenario, including the features previously outlined, constitutes our current understanding of the Universe on large scales and is known as the  $\Lambda$ CDM model [Turner, 1997, Blumenthal et al., 1984]. It is pertinent to emphasize that the cosmological constant  $\Lambda$  represents the simplest theoretical framework in order to explain the observational evidence of an accelerating Universe.

The success of the  $\Lambda$ CDM scenario notwithstanding, it still struggles with the problem of how the particular value of  $\Lambda$  is determined and finely tuned [Perivolaropoulos and Skara, 2022, Condon and Matthews, 2018]. In classical physics, a small value of the cosmological constant  $\Lambda$  does not pose any major problems in theory; it is just another parameter in the theory. However, in Quantum Field Theory (QFT), vacuum fluctuations become crucial, significantly impacting the overall (vacuum) energy density. These issues are at the origin of the challenge known as the "Old Cosmological Constant Problem" [Lombriser, 2019, Weinberg, 1989]. Subsequently, a plethora of different models for dark energy were then proposed to explain the late-time acceleration of the Universe without the cosmological constant, constituting an attempt to fix the fine-tuning problem. They are, in good measure, phenomenological settings that include rolling fields in the presence of a suitable potential; it generalises the cosmological constant through a concrete dynamic behaviour (NB. when the fields are not rolling, their potential energy  $V(\varphi)$  behaves as a cosmological constant [COPELAND et al., 2006]). Let it be added that the main focus has been on spin-zero fields. Moreover, research was also conducted so as to generalise this strategy, employing higher spin dark energy models, such as spinors [Ribas et al., 2005, Cai and Wang, 2008, Yajnik, 2011, Tsyba et al., 2011], vectors [Armendáriz-Picón et al., 1999, Zhao and Zhang, 2006a], and the  $p$ -form field [Koivisto and Nunes, 2009, Gupta, 2011]. Furthermore, alternative explanations for the Universe's late-time acceleration were also constructed, proposing gravitational frameworks beyond General Relativity. E.g., considering modified gravity theories and string-theoretic approaches from quantum gravity [Nojiri and Odintsov, 2003a,b, 2001, 2003c, 2004a,b, 2006a, 2005, Nojiri et al., 2005, Nojiri and Odintsov, 2006b]. Based on the latter proposals, there are current conjectural conditions, as suggested in [Cardone et al., 2004, Paliathanasis and Leon, 2021, Garg and Krishnan, 2019], that have been advocating the construction of new cosmological models with more than one scalar field, aiming at an effective field set-up to be consistent with quantum gravity [Bravo et al., 2020, Achúcarro and Palma, 2019]. Furthermore, concerning information from observational data, it is important to affirm that we do not have unequivocal confirmation of any dynamics beyond the  $\Lambda$ CDM model. However, recent observational data by DESI Collaboration [Collaboration et al., 2024a, Lodha et al., 2024, Calderon et al., 2024] hints at possible deviations, prompting the exploration of models where  $\Lambda$  may not be constant, in an attempt to stretch our outlook beyond the standard model of cosmology. Accordingly, a distinctive and vast literature has explored the dark energy issue, but questions regarding its subtleties remain strong.

Within the broad context that the above paragraphs convey, our specific mindset is Holographic Dark Energy (HDE), proposed by Li [Li, 2004], which stems from the association of an infrared (IR) cut-off of a quantum field theory (QFT) with the Holographic Principle (HP) [Susskind, 1995]. In particular, we continue our research programme promoting and further strengthening an approach that bridges the HP and elements from Fractional Calculus [de Oliveira and Tenreiro Machado, 2014, Miller and Ross, 1993, Grigoletto and Oliveira, 2013]; it was designated as Fractional Holographic Dark Energy (FHDE) and was generically elaborated in [Trivedi et al., 2024], supported with concrete examples of applications. Our main objective in this paper is, therefore, to make progress in investigating whether FHDE can be a realistic and valued contender to explain the late-time accelerated expansion of the universe, in particular, by means of providing concrete field frameworks that can satisfactorily encompass the alluring dynamic properties of FHDE. Within this strategy, we will import features from scalar and gauge fields, suitably assembled into dark energy models while considering the holographic vacuum energy. In more detail, we employ several phenomenological models such as (i) Quintessence, (ii) Kinetic Quintessence (K-essence), (iii) Dilaton, (iv) Yang-Mills condensate, (v) Dirac-Born-Infeld-essence (DBI-essence), and (vi) Tachyon scalar field as favourable inductors of dark energy dynamics. As present in the literature, a considerable number of those models are characterized by having rolling fields because in this way a generalisation of the cosmological constant can be made, by means now of a dynamic behaviour of dark energy i.e., when the fields are not rolling, their potential energy  $V(\varphi)$  behaves as a cosmological constant [COPELAND et al., 2006]. Let us remark again that currently, we do not have the observational data needed to ascertain any dynamics beyond  $\Lambda$ CDM. However, certain data [Collaboration et al., 2024a, Lodha et al., 2024, Calderon et al., 2024] has hinted at possible deviations, prompting the exploration of models in an attempt to stretch our arm beyond the standard model of cosmology.

In our herewith concrete analysis aligned with FHDE, we will consider homogeneous effective field configurations as candidates of dynamical dark energy (cf. (i)-(vi) in the above paragraph), studying their evolution as a function of redshift (or time): this offers the flexibility to probe the late-time cosmic expansion beyond the restrictions of the  $\Lambda$ CDM model by focusing on effective field configurations. Our approach allows for the exploration of a broader set of dark energy models that specifically account for the time-dependent evolution of, for example, the Equation of State (EoS) parameter  $\omega(z)$ , beyond the static framework of  $\Lambda$ CDM model ( $\omega_{\Lambda\text{CDM}} = -1$ ). We, therefore, retrieve an EoS parameter by establishing a correspondence between the FHDE model and effective field configurations as dark energy candidates, followed by presenting plots on the cosmological evolution of the field potential,  $V(\varphi)$ , and the field kinetic energy,  $X$ , over the redshift range  $-1 < z \leq 2$ . Such a holographic reconstruction has been explored in the recent literature, considering several types of cut-off(s), employing different entropic corrections such as Tsallis and Barrows in modified gravity theories (see ref. [Sheykhi, 2011, Zhang, 2007, Wu et al., 2008, Sheykhi, 2010, Karami and Fehri, 2010, Ualikhanova et al., 2024] and [Sharma et al., 2022] for further comments about this procedure). Throughout our paper, we take this idea one step further supported by the lens of the FHDE model [Trivedi et al., 2024], in particular with the Hubble horizon as an IR cut-off by incorporating entropic correction motivated by fractional calculus (see [Jalalzadeh et al., 2021]). Our interest in this problem was majorly motivated by the work in [Sheykhi, 2011, Wu et al., 2008, Sheykhi et al., 2010].

We structure our work as follows. In section 2, we present the choice of IR (infrared) cut-off, within which we define the cosmological evolution of the different dark energy candidates (i)-(vi). Subsequently, in section 3, we derive the EoS parameter along with constructions for the field potential  $V(\varphi)$  and kinetic term  $X$  for various dark energy models. Our results will then be conveyed through the assistance of an adequate plots representing the cosmological evolution for each dark energy candidate over a redshift range of  $-1 < z \leq 2$  for different values of the fractional parameter  $\alpha$  in the range  $1 < \alpha \leq 2$ . We then proceed to section 4, where we discuss our results and provide an outlook for future explorations within the paradigm of the FHDE model.

## 2 Fractional HDE with Hubble horizon as its IR Cut-Off

Before proceeding further, we must choose the cut-off scale  $L$ . As found in the literature, the initial suggestion consisted of taking a cut-off scale given by  $L \rightarrow H^{-1}$ , termed the Hubble horizon cut-off. This choice aimed to alleviate the fine-tuning problem by introducing a natural length scale associated with the inverse of the Hubble parameter,  $H$ , but it was found that this particular scale resulted in the dark energy EoS parameter approaching zero, and it also failed to contribute significantly to the current accelerated expansion of the Universe [Granda and Oliveros, 2008]. An alternative idea that followed was then to consider instead of the particle horizon as the length scale:

$$L_p = a \int_0^t \frac{dt}{a}. \quad (1)$$

Such an alternative yielded an EoS parameter higher than  $-1/3$ , but the challenges of explaining the present acceleration remained unresolved despite this modification. Another line of exploration included the future event horizon as the length scale:

$$L_f = a \int_a^\infty \frac{dt}{a}. \quad (2)$$

Although the desired late-time acceleration regime can be achieved in this case, concerns were raised regarding causality [Kim et al., 2013]. Another option was the Granda-Oliveros cut-off scale, which took into account the derivative of  $H$  into the definition of  $L$  [Granda and Oliveros, 2008]:

$$L_{G-O} = (\alpha H^2 + \beta \dot{H})^{-\frac{1}{2}}. \quad (3)$$

The most generalized proposal for a cut-off is the Nojiri-Odintsov cut-off (see [Nojiri and Odintsov, 2006a, 2017], and [Nojiri et al., 2019] for a detailed review), where we have the following form:

$$L_{N-O} = L(H, \dot{H}, \ddot{H}, \dots, L_p, L_f, \dot{L}_p, \dot{L}_f, \dots). \quad (4)$$

An additional issue with all these cut-off(s) relates to the classical stability of these models against perturbations [Myung, 2007], which is present in all classes of HDE energy densities with various cut-off(s). In general, we can have HDE models where the cut-off could be of the form of a functional as described in Eq. (4), bearing functions of  $H$ ,  $L_p$ , and  $L_f$ . Although all HDEs can be written in the form as described in Eq. (4), it is difficult to motivate any of those cut-off(s) from common physical grounds. This leads to the formulation of various HDE theories being supported by different physical and mathematical considerations. In our work herein, we would like to consider the

Hubble horizon as an IR cut-off. Our reasoning for making this choice is two-fold. On the one hand, we are interested in the simplest way FHDE can produce universal evolution. By universal evolution, we mean that the FHDE model can produce a consistent late-time dark energy behaviour independent of specific assumptions about the cut-off scales, which makes it broadly applicable to various cosmological conditions. In that regard, the Hubble horizon cut-off provides a suitable choice because it is directly related to the local expansion rate of the Universe and avoids issues of causality associated with the event horizon. Its simplicity and direct relevance to current cosmological conditions make it a natural candidate for the FHDE model. On the other hand, the Hubble horizon cut-off has been shown not to work within various HDE frameworks [Li, 2004, Myung, 2007] and so if FHDE can provide an observational consistent scenario then, it would represent a step forward in the ongoing appraisal of the Hubble cut-off. With this in mind, the Hubble cut-off;  $L \rightarrow H^{-1}$  gives:

$$\rho_{\text{de}} = 3c^2 H^{\frac{3\alpha-2}{\alpha}}. \quad (5)$$

We also define the fractional density parameters for dark energy and dark matter as follows:

$$\Omega_{\text{de}} = \frac{\rho_{\text{de}}}{3H^2} \rightarrow c^2 H^{\frac{\alpha-2}{\alpha}}; \quad \Omega_{\text{dm}} = \frac{\rho_{\text{dm}}}{3H^2}. \quad (6)$$

This implies that the Friedman equation takes the following form:

$$\Omega_{\text{de}} + \Omega_{\text{dm}} = 1. \quad (7)$$

The continuity equation for dark energy and dark matter takes the form:

$$\dot{\rho}_{\text{de}} + 3H\rho_{\text{de}}(1 + \omega_{\text{de}}) = 0, \quad (8)$$

$$\dot{\rho}_{\text{dm}} + 3H\rho_{\text{dm}}(1 + \omega_{\text{dm}}) = 0. \quad (9)$$

On algebraic manipulation of Eq. (7) and (9), and Eq. (8) and Eq. (5), we obtain the EoS parameter for the FHDE model as:

$$\omega_{\text{de}} = -1 + \frac{(3\alpha - 2)(1 - \Omega_{\text{de}})}{2\alpha - \Omega_{\text{de}}(3\alpha - 2)}. \quad (10)$$

We use this expression extensively to establish the correspondence between all the effective field configurations and the FHDE model. Note that in the limiting case, when the fractional features start to diminish as  $\alpha \rightarrow 2$ , we find that  $\omega_{\text{de}} \rightarrow 0$ , which is what we usually observe when one considers the conventional HDE scenario:  $\rho_{\text{de}} = 3c^2 H^2$ ; with the Hubble cut-off. The upshot of this discussion is that as the fractional features become more dominant, they play a key role in uncovering the dynamic behaviour of dark energy (see [Trivedi et al., 2024] for a detailed review) during late-time cosmic acceleration of the Universe. Appendix A presents implicit expressions for some of the relevant cosmological parameters, like fractional dark energy density parameter,  $\Omega_{\text{de}}(z)$ , and Hubble parameter,  $H(z)$ , which we will make use in our study as depicted in next section, namely with the assistance of several corroborating plots.

### 3 Reconstructing Fractional Holographic Dark Energy

In this section, we reconstruct the FHDE model for dark energy effective field candidates, such as Quintessence, K-essence, Dilaton, Yang-Mills condensate, Dirac-Born-Infeld-essence, and Tachyons. To be more specific, we establish a correspondence between the FHDE and scalar field models in the following way:

$$\omega_i \leftrightarrow \omega_{\text{de}}, \quad \rho_i \leftrightarrow \rho_{\text{de}}, \quad p_i \leftrightarrow p_{\text{de}}, \quad (11)$$

where, the subscript,  $i$ , acts as the dummy index representing our effective field configuration for establishing the correspondence.

#### 3.1 Quintessence

The most popular alternative to  $\Lambda$  has been the scalar field model of quintessence, which is dynamic, unlike the cosmological constant (see [Steinhardt, 2003]). Several works, such as [Zhang, 2007] and [Wu et al., 2008], have presented an approach to reconstructing dynamical dark energy using a quintessence scalar field with holographic vacuum energy motivated by HP in quantum gravity. The quintessence field has a real-valued scalar field Lagrangian of the form [Tsujikawa, 2013, Zlatev et al., 1999]:

$$\mathcal{L}_{\text{q}} = X_{\text{q}} - V_{\text{q}}(\varphi), \quad (12)$$

where  $X_{\text{q}} \equiv \frac{1}{2}\partial_{\mu}\varphi\partial^{\mu}\varphi$  and  $V_{\text{q}}(\varphi)$  is the field potential. In dynamic scalar field models as quintessence, the potential  $V_{\text{q}}(\varphi)$  takes the role of  $\Lambda$  and must possess some naturalness without fine-tuning. However, the potential receives

quantum loop corrections through a high-energy physics perspective, making it lose its technical naturalness [de Putter and Linder, 2007].<sup>4</sup> In this section, we present the correspondence between the FHDE model and the quintessence scalar field by using the Eq. (11). In this manner, we obtain the fractional holographic reconstructed expressions for the kinetic,  $X_q$ , and potential energy,  $V_q(\varphi)$ , of quintessence with the flat FRW metric. We begin with the action for a quintessence scalar field that reads as:

$$\mathcal{S}_q = \int d^4x \sqrt{-g} \left[ -\frac{1}{2} g^{\mu\nu} \partial_\mu \varphi \partial_\nu \varphi - V_q(\varphi) \right], \quad (13)$$

where  $g^{\mu\nu}$  is the inverse of the metric  $g_{\mu\nu} = \text{diag}(-, +, +, +)$  such that the quintessence field has standard kinetic form. From here, we find the corresponding energy-stress-momentum tensor using the following expression:

$$T_q^{\mu\nu} = \frac{\partial \mathcal{L}_q}{\partial (\partial_\mu \varphi)} \partial^\nu \varphi - g^{\mu\nu} \mathcal{L}_q. \quad (14)$$

By using the Eq. (14) for the quintessence scalar field Lagrangian, the pressure and energy density can be obtained as:

$$\rho_q(t) = \frac{1}{2} \dot{\varphi}_q^2 + V_q(\varphi) \quad \text{and} \quad p_q(t) = \frac{1}{2} \dot{\varphi}_q^2 - V_q(\varphi).$$

From this, and using the expressions for the energy and pressure densities as usual, the EoS parameter is found to be:

$$\omega_q = \frac{p_q}{\rho_q} = \frac{X_q - V_q(\varphi)}{X_q + V_q(\varphi)}. \quad (15)$$

Here  $X_q = \dot{\varphi}_q^2/2$ . Comparing the FHDE EoS parameter (see Eq. (10)) with the EoS parameter of the quintessence scalar field (see Eq. (15)),  $\omega_{\text{de}} = \omega_q$ , we can subsequently write:

$$\frac{X_q - V_q(\varphi)}{X_q + V_q(\varphi)} = -1 + \frac{(3\alpha - 2)(1 - \Omega_{\text{de}})}{2\alpha - \Omega_{\text{de}}(3\alpha - 2)}. \quad (16)$$

Upon algebraic manipulation of the above-written equation, we obtain the following expressions for  $X_q$  and scalar field potential  $V_q(\varphi)$  as:

$$X_q = \frac{\dot{\varphi}_q^2}{2} = \frac{3\Omega_{\text{de}}H^2(3\alpha - 2)(1 - \Omega_{\text{de}})}{4\alpha - \Omega_{\text{de}}(6\alpha - 4)}, \quad (17)$$

$$V_q(\varphi) = 3H^2\Omega_{\text{de}} \left[ 1 - \frac{(3\alpha - 2)(1 - \Omega_{\text{de}})}{4\alpha - 2\Omega_{\text{de}}(3\alpha - 2)} \right]. \quad (18)$$

Eq. (17) and Eq. (18) describe the evolution of the kinetic energy,  $X_q$ , and potential energy,  $V_q(\varphi)$ , of the quintessence field, respectively, with a varying redshift parameter  $z$  in correspondence with the FHDE model. This evolution is illustrated in Figure 1.

With detail:

- In Figure 1a and Figure 1b, we can remark that  $X_q$ , and  $V_q(\varphi)$ , of the quintessence field in fractional holographic reconstruction, decays asymptotically, approaching zero as the redshift  $z$  decreases into the far-future limit  $z \rightarrow -1$ .

In essence, let us then highlight the following:

- This behaviour is consistent across all values of the fractional parameter  $\alpha$ .
- For larger values of  $\alpha$  (e.g.,  $\alpha = 1.8$  and  $1.6$ ),  $X_q$  and  $V_q(\varphi)$  shows a highly dynamic evolution<sup>5</sup>.
- In contrast, the evolution is less dynamic for smaller values of  $\alpha$  (e.g.,  $\alpha = 1.4$  and  $1.2$ ).

<sup>4</sup>An alternative approach is adopting non-canonical kinetic terms in the scalar field Lagrangian, leading to a model known as Kinetic Quintessence (K-essence), which we will discuss in more detail in the next subsection.

<sup>5</sup>By highly dynamic evolution, we mean that the evolution of the field changes more rapidly and the contrary for less dynamic evolution as we approach far-future limit  $z \rightarrow -1$ .

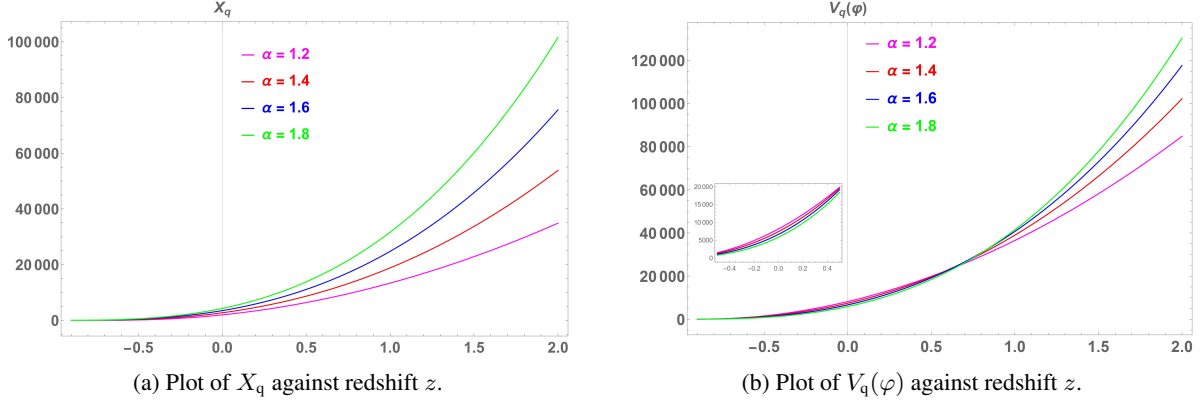


Figure 1: Plot for  $X_q$  and  $V_q(\varphi)$  against redshift  $z$  for  $\alpha = 1.2, 1.4, 1.6$  and  $1.8$ .

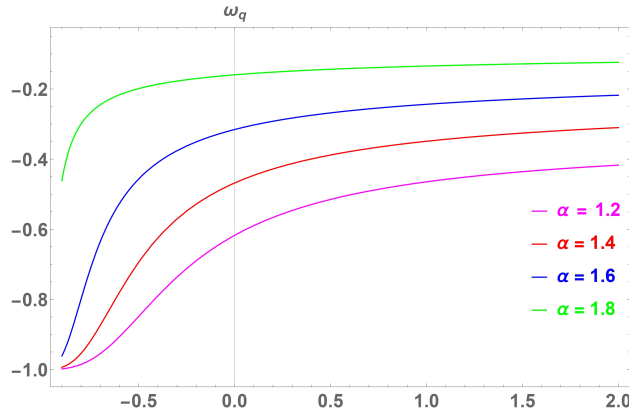


Figure 2: Plot of  $\omega_q$  against redshift  $z$  for  $\alpha = 1.2, 1.4, 1.6$  and  $1.8$ ; here  $c = 0.01$ .

- However, as the redshift decreases below  $z < 0.55$  (see in Figure 1b), subtle differences in the behaviour of the potential emerge, with  $\alpha = 1.8$  showing more appropriateness<sup>6</sup> due to its less dynamic evolution as the Universe transitions to a dark energy-dominated phase. As  $z \rightarrow -1$ , the kinetic and potential energies tend to zero asymptotically, approaching a  $\Lambda$ CDM behaviour.
- In Figure 2, we plotted the EoS parameter,  $\omega_q$ , of the fractional holographic reconstructed quintessence model. A suitable evolution of  $w_q \rightarrow -1$  is possible to be retrieved: we identify that as fractional features start to dominate i.e., for small values of  $\alpha$ , like  $\alpha = 1.2$  and  $1.4$ , the EoS parameter for the quintessence scalar field asymptotically approaches to the  $\Lambda$ CDM behaviour:  $\omega_{\Lambda\text{CDM}} = -1$ , during the dark energy-dominated phase. As larger values of  $\alpha$  are considered, the  $\omega_q$  values deviate more from the  $\Lambda$ CDM behaviour. We note that for  $\alpha$  from  $\alpha = 1.2$  to  $1.8$ , the evolution of  $\omega_q$  remains in the quintessence regime  $-1 < \omega_q < -1/3$  during far-future limit  $z \rightarrow -1$ .

Summarising for this subsection, Figure 1a suggests that higher values of  $\alpha$  may not be suitable because they do not ensure a slow evolving field, not matching a nearly constant dark energy behaviour. On the other hand, in Figure 1b, a higher value for  $\alpha$  is preferable (over smaller values) because it induces a suitable situation for the potential for redshift region  $-1 < z < 0.55$ .

### 3.2 K-essence

A useful manner to consider Kinetic quintessence, typically abbreviated as K-essence, where "K" stands for Kinetic, is a generalisation of the scalar field model with a standard kinetic term, i.e. common quintessence. Unlike in Quintessence, the K-essence scalar field framework avoids the requirement of a field potential, hence attempting to

<sup>6</sup>The most appropriate model should ensure  $V_q \gg X_q$  even at late-times. The potential reduces more gradually for  $\alpha = 1.8$ , ensuring  $\omega_q$  remains close to  $-1$  for an extended period.

evade loop corrections in high-energy physics. K-essence scalar field has a Lagrangian of the form:

$$\mathcal{L}_{\text{kq}} = f_{\text{kq}}(\varphi)F(X) - V(\varphi). \quad (19)$$

From Eq. (19), the Lagrangian for a scalar field with the standard kinetic term can be obtained by setting  $f_{\text{kq}}(\varphi) = 1$  and  $F(X) = X$ , i.e. quintessence. The primary aim of the k-essence model is to describe the inflationary evolution in the absence of a potential by employing a general class of non-standard kinetic terms for a scalar field  $\varphi$ . In [Armendáriz-Picón et al., 1999], the authors consider a general kinetic Lagrangian  $P(\varphi, X_{\text{kq}})$  for K-essence models to have relevance to a large class of models, which consists of the scalar field  $\varphi$  and  $X_{\text{kq}} = -\dot{\varphi}_{\text{kq}}^2/2$ . The action for K-essence can be written as:

$$\mathcal{S}_{\text{kq}} = \int d^4x \sqrt{-g} P(\varphi, X_{\text{kq}}). \quad (20)$$

Its corresponding energy-stress-momentum tensor provides us with the energy density  $\rho_{\text{kq}}(\varphi, X_{\text{kq}})$  and pressure  $p_{\text{kq}}(\varphi, X_{\text{kq}})$ , which can be expressed as shown in [Armendáriz-Picón et al., 1999, Copeland et al., 2006]:

$$\rho_{\text{kq}}(\varphi, X_{\text{kq}}) = f_{\text{kq}}(\varphi) (-X_{\text{kq}} + 3X_{\text{kq}}^2) \quad \text{and} \quad p_{\text{kq}}(\varphi, X_{\text{kq}}) = f_{\text{kq}}(\varphi) (-X_{\text{kq}} + X_{\text{kq}}^2).$$

Here, the function  $f_{\text{kq}}(\varphi)$  represents the nature of coupling with the scalar field (for a detailed review, see [Armendáriz-Picón et al., 1999]). Moreover, we calculate its EoS parameter  $\omega_{\text{kq}} = p_{\text{kq}}/\rho_{\text{kq}}$ . We obtain:

$$\omega_{\text{kq}} = \frac{X_{\text{kq}} - 1}{3X_{\text{kq}} - 1}. \quad (21)$$

Comparing the FHDE EoS parameter (see Eq. (10)) with the EoS parameter of the k-essence scalar field (see Eq. (21)). We obtain:

$$\frac{X_{\text{kq}} - 1}{3X_{\text{kq}} - 1} = -1 + \frac{(3\alpha - 2)(1 - \Omega_{\text{de}})}{2\alpha - \Omega_{\text{de}}(3\alpha - 2)} \quad (22)$$

Upon algebraic manipulation of the above-written equation, we obtain the following expressions for  $X_{\text{kq}}$  and  $f_{\text{kq}}(\varphi)$  as:

$$X_{\text{kq}} = -\frac{\dot{\varphi}_{\text{kq}}^2}{2} = 1 - \frac{2(\alpha - 2)}{\alpha(1 + 3\Omega_{\text{de}}) - 2(\Omega_{\text{de}} + 3)}, \quad (23)$$

$$f_{\text{kq}}(\varphi) = \frac{3H^2\Omega_{\text{de}}(\alpha + 3\alpha\Omega_{\text{de}} - 2(3 + \Omega_{\text{de}}))^2}{2(2 + \alpha + 2\Omega_{\text{de}} - 3\alpha\Omega_{\text{de}})(\alpha(3\Omega_{\text{de}} - 2) - 2\Omega_{\text{de}})}. \quad (24)$$

Eq. (23) and Eq. (24) describe the late-time cosmic evolution of the kinetic energy,  $X_{\text{kq}}$ , and coupling function,  $f_{\text{kq}}$ , respectively, with a varying redshift parameter  $z$  in correspondence with the FHDE model. This evolution is illustrated in Figure 2.

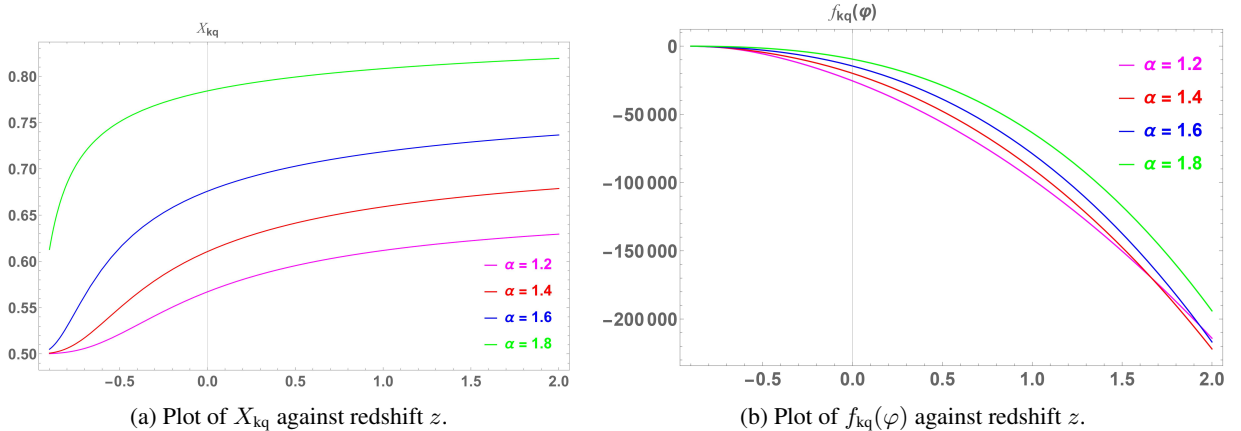


Figure 3: Plot for  $X_{\text{kq}}$  and  $f_{\text{kq}}(\varphi)$  against redshift  $z$  for  $\alpha = 1.2, 1.4, 1.6$  and  $1.8$ .

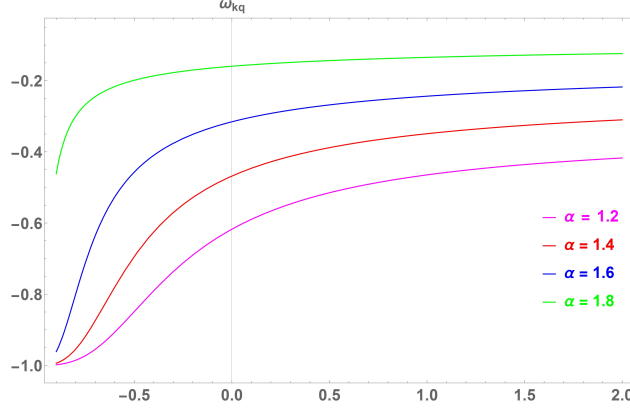


Figure 4: Plot of  $\omega_{kq}$  against redshift  $z$  for  $\alpha = 1.2, 1.4, 1.6$  and  $1.8$ ; here  $c = 0.01$ .

We notice the following:

- In Figure 3a and Figure 3b, we can observe that the kinetic energy,  $X_{kq}$ , and the coupling function,  $f_{kq}(\varphi)$ , of the K-essence field in fractional holographic reconstruction, decays asymptotically, approaching  $X_{kq} \rightarrow 1/2$ , and  $f_{kq}(\varphi) \rightarrow 0$  as the redshift  $z$  decreases in far-future limit  $z \rightarrow -1$ .

In particular:

- For larger values of  $\alpha$  (e.g.,  $\alpha = 1.8$  and  $1.6$ ),  $X_{kq}$  shows a highly dynamic (or faster) evolution as redshift  $z$  decreases.
- In contrast, the evolution is less dynamic (or slower) for smaller values of  $\alpha$  (e.g.,  $\alpha = 1.4$  and  $1.2$ ) as redshift  $z$  decreases.
- On the other hand, in Figure 3b, we can remark that  $f_{kq}(\varphi)$  increases from a smaller value at high redshifts to asymptotically approach zero at low redshifts. For larger values of  $\alpha$ , (e.g.,  $\alpha = 1.8$  and  $1.6$ ),  $f_{kq}(\varphi)$  less dynamic (or slower) evolution is observed with decreasing redshift, whereas the evolution for smaller values of  $\alpha$  (e.g.,  $\alpha = 1.2$  and  $1.4$ ), highly dynamic over the redshift region  $-1 < z \leq 2$ .
- In Figure 4, we plotted for the EoS parameter,  $\omega_{kq}$ , of the fractional holographic reconstructed K-essence model. A suitable evolution of  $\omega_{kq} \rightarrow -1$  is possible to be retrieved: we identify that as fractional features start to dominate i.e., for small values of  $\alpha$ , like  $\alpha = 1.2$  and  $1.4$ , the EoS parameter for K-essence scalar field asymptotically approaches to the  $\Lambda$ CDM behaviour, during dark energy dominated phase. We observe a similar behaviour for the EoS parameter for quintessence (see Figure 2) in the far-future limit.

To sum up, Figure 3a suggests that higher values of  $\alpha$  may not be suitable because they do not ensure a slow evolution of the field, as we remarked for Quintessence, in Figure 3a. Therefore, higher values of  $\alpha$  do not seem suitable, to match a nearly constant dark energy behaviour.

### 3.3 Dilaton

Dilatonic Ghost condensate is a new type of dark energy model based on String Theory. In [Piazza and Tsujikawa, 2004], the authors consider the classical dynamics of the system with a negative kinematic term  $-X$  and the bell-type potential and estimate the result that the dilaton field evolves toward the potential maximum with an EoS:  $\omega_d \leq -1$ . However, since this system is unstable due to quantum fluctuations, a term of the type,  $\exp(\lambda\varphi)X^2$ , ensures stability at the quantum scale. When the conditions for the stability are satisfied, the EoS is restricted in the range from being greater than or equal to  $-1$  in sharp contrast to the phantom field models of dark energy, as discussed in [Carroll et al., 2003]. The most general form of Lagrangian for a scalar field can be expressed as:

$$\mathcal{L}_d = \frac{1}{2}(\partial\varphi)^2 + \frac{A}{m^4}(\partial\varphi)^4 \exp\left(\frac{\lambda\varphi}{M_P}\right) + \text{higher order terms.} \quad (25)$$

Hereafter, we will set the Planck mass to unity and express the Lagrangian as:

$$p_d(X_d, \varphi) = -X_d + \beta \exp(\lambda\varphi)X_d^2, \quad (26)$$



where  $\beta = A/m^4$ . The energy-stress-momentum tensor for this Lagrangian can be expressed as:

$$T_{\mu\nu}^{\varphi} = g_{\mu\nu}p_d + \frac{\partial p_d}{\partial X} \partial_{\mu}\varphi \partial_{\nu}\varphi. \quad (27)$$

From this, the energy density can be obtained as:

$$\rho_d(X, \varphi) = -X + 3\beta \exp(\lambda\varphi)X^2 \quad (28)$$

where,  $X_d = \dot{\varphi}^2/2$ , and  $\lambda$ , and  $\beta$  are constants. The EoS parameter for the dilaton model can be written as:

$$\omega_d = \frac{-1 + \beta \exp(\lambda\varphi)X_d}{-1 + 3\beta \exp(\lambda\varphi)X_d}. \quad (29)$$

Now, we establish the correspondence between the FHDE EoS parameter and the Dilaton EoS parameter, and we obtain:

$$\frac{-1 + \beta \exp(\lambda\varphi)X_d}{-1 + 3\beta \exp(\lambda\varphi)X_d} = -1 + \frac{(3\alpha - 2)(1 - \Omega_{de})}{2\alpha - \Omega_{de}(3\alpha - 2)} \quad (30)$$

Upon solving the above-written equation we obtain the expression for  $X_d$ , and  $\beta \exp(\lambda\varphi)X_d$  as:

$$X_d = \frac{\dot{\varphi}^2}{2} = \frac{3H^2\Omega_{de}(\alpha + 3\alpha\Omega_{de} - 2(3 + \Omega_{de}))}{\alpha(6\Omega_{de} - 4) - 4\Omega_{de}}, \quad (31)$$

$$\beta \exp(\lambda\varphi)X_d = 1 - \frac{2(\alpha - 2)}{\alpha + 3\alpha\Omega_{de} - 2(3 + \Omega_{de})}. \quad (32)$$

Eq. (31) and Eq. (32) describe the late-time cosmic evolution of kinetic energy,  $X_d$ , and exponential potential,  $\beta \exp(\lambda\varphi)X_d$ , with varying redshift parameter  $z$  in correspondence with the FHDE model. The evolution is illustrated in Figure 5.

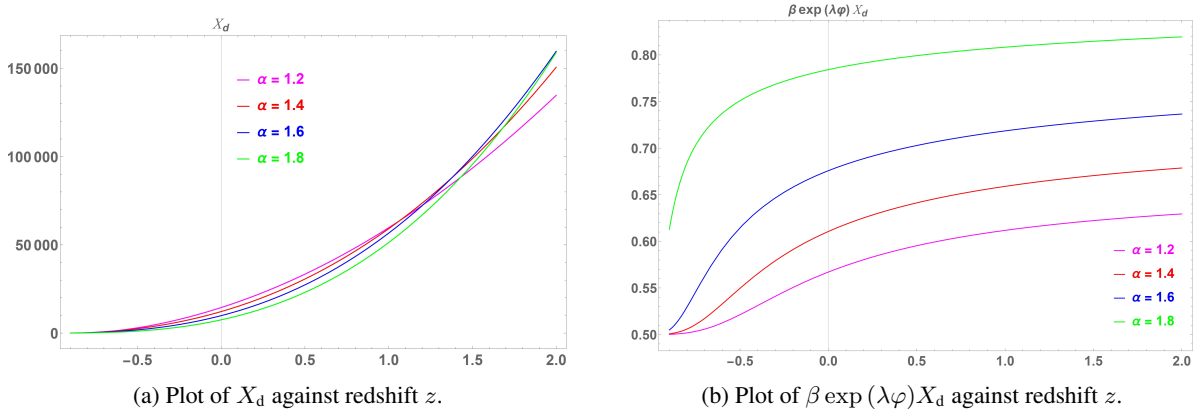


Figure 5: Plot of  $X_d$  and  $\beta \exp(\lambda\varphi)X_d$ , respectively, against redshift  $z$  for  $\alpha = 1.2, 1.4, 1.6$  and  $1.8$ .

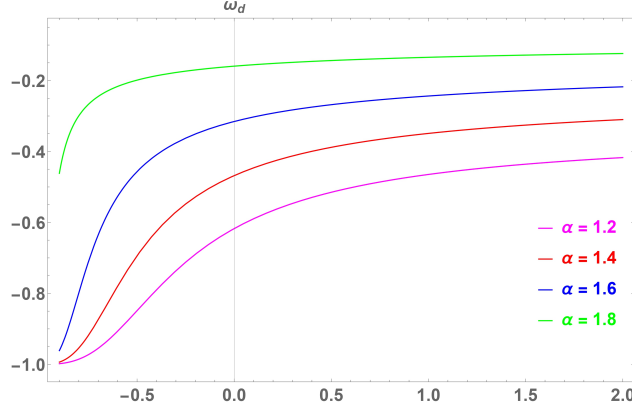


Figure 6: Plot of  $\omega_d$  against redshift  $z$  for  $\alpha = 1.2, 1.4, 1.6$  and  $1.8$ ; here  $c = 0.01$ .

With detail:

- In Figure 5a and Figure 5b, we observe that the kinetic energy,  $X_d$ , and the exponential function,  $\beta \exp(\lambda\varphi)X_d$ , of the Dilaton field in fractional holographic reconstruction decay asymptotically, approaching  $X_d \rightarrow 0$ , and  $\beta \exp(\lambda\varphi)X_d \rightarrow 1/2$ , respectively, as the redshift  $z$  decreases in the far-future limit  $z \rightarrow -1$ .

In addition, we can notice the following:

- For larger values of  $\alpha$  (e.g.,  $\alpha = 1.8$  and  $1.6$ ),  $X_d$  shows a highly dynamic (or faster) evolution, whereas the evolution is less dynamic (or slower) for smaller values of  $\alpha$  (e.g.,  $\alpha = 1.4$  and  $1.2$ ) in the redshift region  $1.5 \leq z \leq 2$ .
- As we take smaller and smaller values of redshift in the far-future limit  $z \rightarrow -1$ , a less dynamic behaviour is perceived for large values of  $\alpha$  and a highly dynamic behaviour for smaller values of  $\alpha$ .
- On the other hand, in Figure 5b, we discern that for larger values of  $\alpha$  (e.g.,  $\alpha = 1.8$  and  $1.6$ ), the potential evolution is highly dynamical (or faster) and in contrast, the evolution for smaller values of  $\alpha$  (e.g.,  $\alpha = 1.2$  and  $1.4$ ), is less dynamic over the redshift region  $-1 < z \leq 2$ .
- In Figure 6, we plotted for the EoS parameter,  $\omega_d$ , of the fractional holographic reconstructed Dilaton model. We can retrieve that a suitable evolution of  $\omega_d \rightarrow -1$  is possible to identify as fractional features start to dominate because it represents a scenario where the K-essence scalar field behaves similarly to the  $\Lambda$ CDM model during dark energy dominated phase.

We observe a similar behaviour for the EoS parameter for quintessence (see Figure 2) and K-essence (see Figure 4) in the far-future limit.

In a nutshell, Figure 5a suggests that a higher value of  $\alpha$  provides a suitable scenario because it ensures a slow-evolving field, making it suitable to fit with a nearly constant dark energy behaviour. On the other hand, in Figure 5b, a lower value of  $\alpha$  is preferable (over larger values) because it induces a suitable situation<sup>7</sup> for the potential in the redshift region  $-1 < z \leq 2$ .

### 3.4 Yang-Mills Field condensate

The Yang-Mills Condensate (YMC) is an interesting approach to the problem of dark energy. It involves studying gauge boson fields in cosmological settings to investigate the cosmic evolution of components such as dark energy. The motivation for investigating YMC alongside the dynamic scalar field theories as a possible dark energy candidate is two-fold. First, the effective Yang-Mills Lagrangian is entirely determined by quantum field theory, which implies that the only parameter that can be changed is the energy scale of the theory. Thus, any modifications to the effective Lagrangian of the theory should be avoided. Second, in scalar field dark energy models such as quintessence, the EoS parameter lies in the range  $-1 < \omega_q < 1$ . In order to obtain  $\omega_q < -1$ , one needs to introduce a "phantom" field, which may bear quantum instabilities. However, that is avoided in the YMC dark energy model (see [Zhao and Zhang, 2006a] and [Zhao et al., 2009] for a review).

<sup>7</sup>We retrieve that the exponential potential of Dilaton,  $\beta \exp(\lambda\varphi)X_d$ , behaves similarly to  $X_{kq}$  (see Figure 3a) and approaches a value of  $1/2$  in the far-future limit  $z \rightarrow -1$ .

In an effective YMC dark energy model, the Lagrangian is given by [Zhao and Zhang, 2006a, Adler, 1981, Zhao and Zhang, 2006b] as,

$$\mathcal{L}_{\text{YMC}} = \frac{b}{2} F \left( \ln \left| \frac{F}{\kappa^2} \right| - 1 \right), \quad (33)$$

where  $\kappa$  is the renormalisation scale of the dimension of squared mass,  $b$  is Callan-Symanzik coefficient  $b = (11N - 2N_f)/24\pi^2$  for  $SU(N)$  where  $N_f$  represents the number of quark flavours, and  $F \equiv -\frac{1}{2}F_{\mu\nu}^a F^{a\mu\nu}$  plays the role of the order parameter of the YMC. The index  $a$  runs over the gauge group, for example,  $a = 1, 2, 3$  for  $SU(2)$ ,  $a = 1, 2, 3, \dots, 8$  for  $SU(3)$ . Let us consider the ideal scenario where the only component in the Universe is YMC, which is minimally coupled to gravity. The effective action becomes,

$$S_{\text{YMC}} = \int d^4x \sqrt{-g} \left[ \frac{\mathcal{R}}{16\pi G} + \frac{b}{2} F \left( \ln \left| \frac{F}{\kappa^2} \right| - 1 \right) \right]. \quad (34)$$

On applying the variational principle on the action with respect to the metric  $g^{\mu\nu}$ , we obtain the Einstein equation  $G_{\mu\nu} = 8\pi G T_{\mu\nu}$ . The energy-stress-momentum tensor can be written as,

$$T_{\mu\nu} = \sum_{a=1}^3 \frac{g_{\mu\nu}}{4g^2} F_{\sigma\delta}^a F^{a\sigma\delta} + \epsilon F_{\mu\nu}^a F_{\nu}^{a\sigma}, \quad (35)$$

Herewith, we assume that the gauge fields are only the functions of time<sup>8</sup>. They can be expressed as  $A_\mu = \frac{i}{2} \sigma_a A_\mu^a(t)$ , where  $\sigma_a$  are Pauli's matrices. The time component and the spatial component can be written as  $A_0 = 0$  and  $A_i^a = \delta_i^a(t)$ , respectively. The Yang-Mills field tensor is defined as usual,

$$F_{\mu\nu}^a = \partial_\mu A_\nu^a - \partial_\nu A_\mu^a + g f^{abc} A_\mu^b A_\nu^c, \quad (36)$$

where  $f^{abc}$  is the structure constant of the group. Here, the dielectric constant is defined by  $\epsilon = 2\partial\mathcal{L}_{\text{YMC}}/\partial F$ . We get,

$$y = \frac{\epsilon}{b} = \ln \left| \frac{F}{\kappa^2} \right|. \quad (37)$$

Now, let us find the corresponding energy density and pressure of the energy-stress-momentum tensor in Eq. (35). We obtain,

$$\rho_{\text{YMC}} = \frac{1}{2} \epsilon (E^2 + B^2) + \frac{1}{2} b (E^2 - B^2) \quad \text{and} \quad p_{\text{YMC}} = \frac{1}{6} \epsilon (E^2 + B^2) - \frac{1}{2} b (E^2 - B^2).$$

Since, for an expanding Universe, the magnetic component of the Yang-Mills field falls off much faster, and the field effectively becomes the electric type as suggested in [ZHAO and XU, 2007]. This consideration simplifies the expressions of energy density and pressure in the following way,

$$\rho_{\text{YMC}} = \frac{E^2}{2} (\epsilon + b) \quad \text{and} \quad p_{\text{YMC}} = \frac{E^2}{2} \left( \frac{\epsilon}{3} - b \right).$$

We find it convenient to simplify the expressions further by introducing a dimensionless quantity, which we established earlier in Eq. (37). Thereby, further modifying the expressions into the following form,

$$\rho_{\text{YMC}} = \frac{1}{2} b \kappa^2 (y + 1) \exp(y) \quad \text{and} \quad p_{\text{YMC}} = \frac{1}{6} b \kappa^2 (y - 3) \exp(y).$$

The EoS of Yang-Mills Condensate becomes,

$$\omega_{\text{YMC}} = \frac{y - 3}{3y + 3}. \quad (38)$$

Now, finally establishing the correspondence with the FHDE model in the following manner,

$$\frac{y - 3}{3y + 3} = -1 + \frac{(3\alpha - 2)(1 - \Omega_{\text{de}})}{2\alpha - \Omega_{\text{de}}(3\alpha - 2)}. \quad (39)$$

<sup>8</sup>A broad discussion on suitable ansatz for the gauge fields can be found in [Moniz and Mourao, 1991, Moniz et al., 1993].

On solving, we obtain,

$$E^2 = \kappa^2 \exp\left(3 - \frac{12(\alpha - 2)}{\alpha + 3\alpha\Omega_{\text{de}} - 2(3 + \Omega_{\text{de}})}\right). \quad (40)$$

Eq. (40) describes the late-time cosmic evolution of the YMC field, which ultimately takes the form of an electric field due to the approximations taken into account to address the late-time Universe as a function of the redshift parameter. The YMC field configuration is particularly different from the rest of the effective field candidates due to the spin-1 gauge fields governing it in a cosmological setting. We plot the evolution of the electric field as shown in Figure 7a. Furthermore, we plot the EoS parameter in Figure 7b.

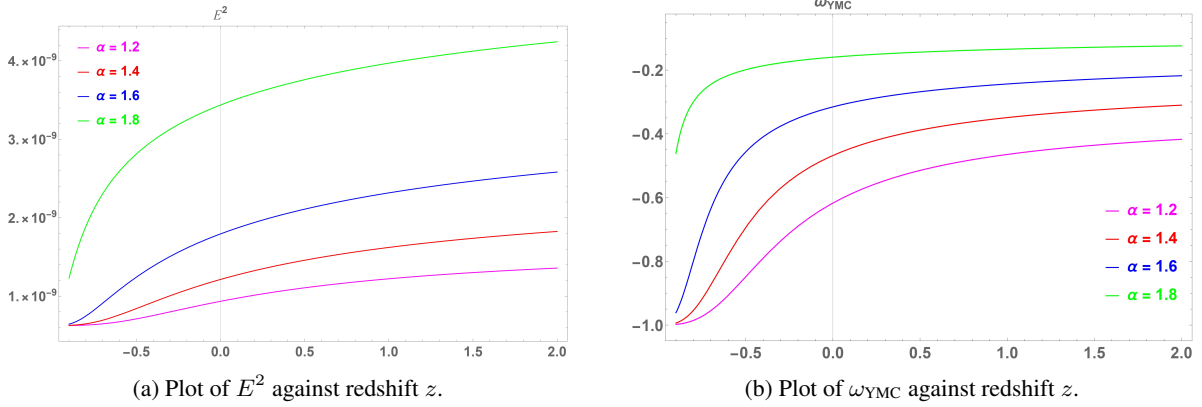


Figure 7: Plot for  $E^2$  and  $\omega_{\text{YMC}}$  against redshift  $z$  for  $\alpha = 1.2, 1.4, 1.6$  and  $1.8$ .

In particular:

- In Figure 7a, we observe that the electric component,  $E^2$ , of the YMC field in fractional holographic reconstruction, decays asymptotically to approach  $E^2 \rightarrow 0$  as the redshift  $z$  decreases in the far-future limit  $z \rightarrow -1$ .

Furthermore, for larger values of  $\alpha$  (e.g.,  $\alpha = 1.8$  and  $1.6$ ),  $E^2$  shows a highly dynamic evolution, whereas the evolution is less dynamic for smaller values of  $\alpha$  (e.g.,  $\alpha = 1.4$  and  $1.2$ ) in the redshift region  $-1 < z \leq 2$ .

- On the other hand, in Figure 7b, we plotted for the EoS parameter,  $\omega_{\text{YMC}} \rightarrow -1$  and is possible to identify that as fractional features start to dominate, it conveys a scenario where the YMC field behaves similarly to the  $\Lambda$ CDM model during dark energy dominated phase.

We remark a similar behaviour for the EoS parameter for quintessence (see Figure 2), K-essence (see Figure 4) and Dilaton (see Figure 6).

Thus, Figure 7a suggests that higher values of  $\alpha$  may not be suitable because they do not ensure a slow evolving field, making it inadequate for a nearly constant dark energy.

### 3.5 DBI-essence Field

Recent works in String Theory propose intriguing scenarios where the inflaton, central to inflationary cosmology, is identified with the separation between two branes navigating extra dimensions within a warped throat. This interpretation arises naturally from the action of the system, which is proportional to the volume swept out by the brane as it moves. The volume, determined by the square root of the induced metric, inherently generates a Dirac–Born–Infeld (DBI) kinetic term, linking this framework directly to the inflationary phase of rapid expansion in the early Universe (see [Ahn et al., 2009] for more details). Let us herewith consider the DBI scalar field as the dark energy whose action reads as:

$$\mathcal{S}_{\text{DBI}} = - \int d^4x a^3(t) \left[ T(\varphi) \sqrt{1 - \frac{\dot{\varphi}^2}{T(\varphi)}} + V(\varphi) - T(\varphi) \right], \quad (41)$$

where  $T(\varphi) = n\dot{\varphi}^2$  represents the warped brane tension, but we will refer to it as the kinetic energy  $X_{\text{DBI}}$ , and  $V(\varphi)$  is the potential arising from interactions with the Ramond-Ramond fluxes (see [Silverstein and Tong, 2004]). We then

proceed to obtain the energy density and pressure expressions as:

$$\rho_{\text{DBI}} = (\eta - 1)T(\varphi) + V(\varphi) \quad \text{and} \quad p_{\text{DBI}} = \left(\frac{\eta - 1}{\eta}\right)T(\varphi) - V(\varphi).$$

Here,  $\eta$  represents the Lorentz Boost factor, which can be written as:

$$\eta = \sqrt{\frac{1}{1 - \dot{\varphi}^2/T(\varphi)}}. \quad (42)$$

Moreover, the EoS parameter for DBI-essence dark energy can be written as:

$$\omega_{\text{DBI}} = \frac{(\eta - 1)T(\varphi) - \eta V(\varphi)}{\eta(\eta - 1)T(\varphi) + \eta V(\varphi)}. \quad (43)$$

Now, we are establishing the correspondence with the FHDE model. We obtain:

$$\frac{(\eta - 1)T(\varphi) - \eta V(\varphi)}{\eta(\eta - 1)T(\varphi) + \eta V(\varphi)} = -1 + \frac{(3\alpha - 2)(1 - \Omega_{\text{de}})}{2\alpha - \Omega_{\text{de}}(3\alpha - 2)}. \quad (44)$$

Upon solving the above-written correspondence equation, we obtain the expressions for  $X_{\text{DBI}}$  and  $V_{\text{DBI}}(\varphi)$  as:

$$X_{\text{DBI}} = n\dot{\varphi}_{\text{DBI}}^2 = \frac{3(3\alpha - 2)H^2(n - 1)\sqrt{\frac{n}{n-1}}(1 - \Omega_{\text{de}})\Omega_{\text{de}}}{2\alpha - (3\alpha - 2)\Omega_{\text{de}}}, \quad (45)$$

$$V_{\text{DBI}}(\varphi) = 3H^2\Omega_{\text{de}} - \frac{3(3\alpha - 2)H^2(n - 1)\sqrt{\frac{n}{n-1}}\left(\sqrt{\frac{n}{n-1}} - 1\right)(1 - \Omega_{\text{de}})\Omega_{\text{de}}}{2\alpha - (3\alpha - 2)\Omega_{\text{de}}}. \quad (46)$$

Eq. (45) and Eq. (46) describe the late-time cosmic evolution of the kinetic energy,  $X_{\text{DBI}}(\varphi)$ , and potential,  $V_{\text{DBI}}(\varphi)$ , in correspondence with the FHDE model. The evolution is illustrated in Figure 7 and Figure 8.

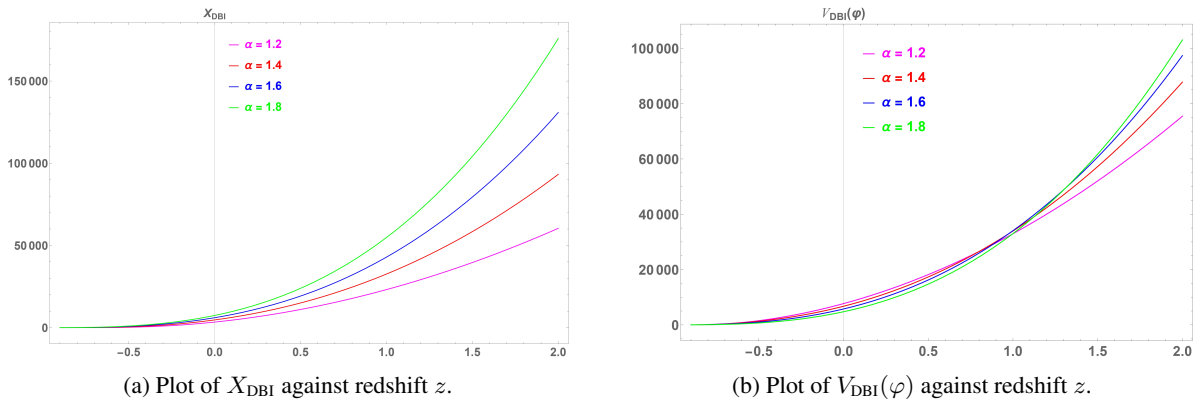


Figure 8: Plot of  $X_{\text{DBI}}$  and  $V_{\text{DBI}}(\varphi)$  against redshift  $z$  for  $\alpha = 1.2, 1.4, 1.6$  and  $1.8$ . Here  $n = 1.5$ .

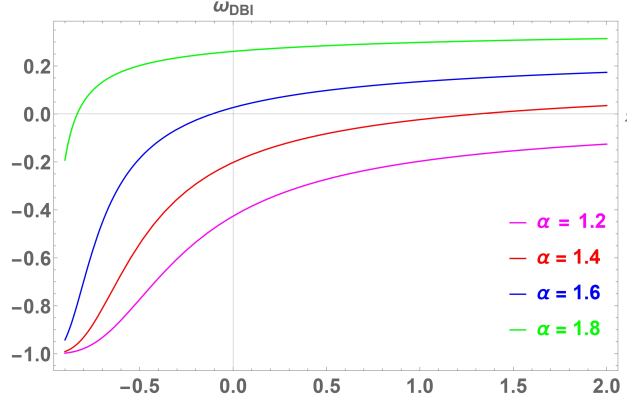


Figure 9: Plot of  $\omega_{\text{DBI}}$  against redshift  $z$  for  $\alpha = 1.2, 1.4, 1.6$  and  $1.8$ ; here  $c = 0.01$ .

We notice the following:

- In Figure 8a and Figure 8b, we notice that the kinetic energy,  $X_{\text{DBI}}$ , and the potential energy,  $V_{\text{DBI}}(\varphi)$ , of the DBI-essence field in fractional holographic reconstruction, decays to asymptotically approach zero, respectively, as the redshift  $z$  decreases in the far-future limit  $z \rightarrow -1$ .

In particular:

- This behaviour of  $X_{\text{DBI}}$  and  $V_{\text{DBI}}(\varphi)$  is consistent across all values of the fractional parameter  $\alpha$ .
- For larger values of  $\alpha$  (e.g.,  $\alpha = 1.8$  and  $1.6$ ), the evolution for  $X_{\text{DBI}}$  shows a highly dynamic evolution, whereas the evolution is less dynamic for smaller values of  $\alpha$  (e.g.,  $\alpha = 1.4$  and  $1.2$ ).
- In Figure 8b, it is noticed a similar behaviour to what we observed in quintessence (see Figure 1a), however, for a different redshift region:  $-1 < z \leq 0.99$ ; where the  $V_{\text{DBI}}(\varphi)$  decreases less dynamically for larger values of  $\alpha$  (e.g.,  $\alpha = 1.8$  and  $1.6$ ).
- In Figure 9, we plotted for the EoS parameter,  $\omega_{\text{DBI}} \rightarrow -1$  and is possible to identify that as fractional features start to dominate, it represents a scenario where the DBI-essence field behaves similarly to the  $\Lambda$ CDM model during dark energy dominated phase. Moreover, the EoS parameter takes a different value at  $z = 0$  from what we observed in Quintessence, K-essence, Dilaton and YMC fields.

In summary regarding this subsection, Figure 8a suggests that a higher value of  $\alpha$  may not provide a suitable scenario because it does not ensure a slow-evolving field, not mimicking a nearly constant dark energy behaviour. On the other hand, in Figure 8b, a higher value of  $\alpha$  is preferable (over smaller values) because it induces a suitable situation for the potential in the redshift region  $-1 < z \leq 0.99$ .

### 3.6 Tachyonic Field

The tachyon field is a possible candidate for inflation and dark energy at high energies as suggested in [Mazumdar et al., 2001, Feinstein, 2002, Piao et al., 2002, Gibbons, 2002]. However, the nature of the potential for self-interaction,  $V(\varphi)$ , acts as a deciding factor to ultimately obtain the desired dark energy behaviour. By setting the correspondence with FHDE, we attempt to express the potential explicitly, which will help us later study the tachyon field's cosmological evolution. We begin with the effective tachyon scalar field Lagrangian,

$$\mathcal{L}_t = -V_t(\varphi) \sqrt{1 - g^{\mu\nu} \partial_\mu \varphi \partial_\nu \varphi} \quad (47)$$

Its corresponding energy-stress-momentum tensor can be written similarly to that of a perfect-fluid tensor in the following way,

$$T_{\mu\nu}^\varphi = (p_t + \rho_t) u_\mu u_\nu + p_t g_{\mu\nu} \quad (48)$$

The energy density and pressure can be written as,

$$p_t(t) = -V_t(\varphi) \sqrt{1 - \dot{\varphi}_t^2} \quad \text{and} \quad \rho_t(t) = \frac{V_t(\varphi)}{\sqrt{1 - \dot{\varphi}_t^2}}. \quad (49)$$

Moreover, the EoS parameter can be expressed as,

$$\omega_t = \dot{\varphi}_t^2 - 1. \quad (50)$$

Now, establishing the correspondence with FHDE provides us with

$$\dot{\varphi}_t^2 - 1 = -1 + \frac{(3\alpha - 2)(1 - \Omega_{\text{de}})}{2\alpha - \Omega_{\text{de}}(3\alpha - 2)}. \quad (51)$$

Upon solving the above-written correspondence equation, we obtain the expression for  $\dot{\varphi}_t$  and  $V_t(\varphi)$  as,

$$X_t = \frac{\dot{\varphi}_t^2}{2} = \frac{(3\alpha - 2)(1 - \Omega_{\text{de}})}{4\alpha - \Omega_{\text{de}}(6\alpha - 4)}, \quad (52)$$

$$V_t(z) = 3H^2\Omega_{\text{de}} \cdot \left[ 1 - \frac{(3\alpha - 2)(1 - \Omega_{\text{de}})}{2\alpha - \Omega_{\text{de}}(3\alpha - 2)} \right]^{\frac{1}{2}}. \quad (53)$$

Let us now elaborate on this setting, starting with the following plots.

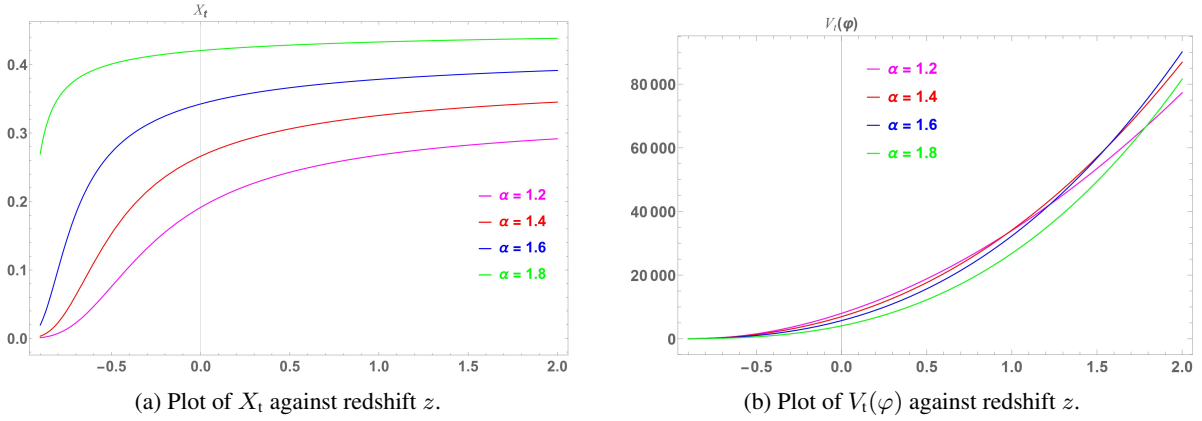


Figure 10: Plot of  $X_t$  and  $V_t(\varphi)$  against redshift  $z$  for  $\alpha = 1.2, 1.4, 1.6$  and  $1.8$ .

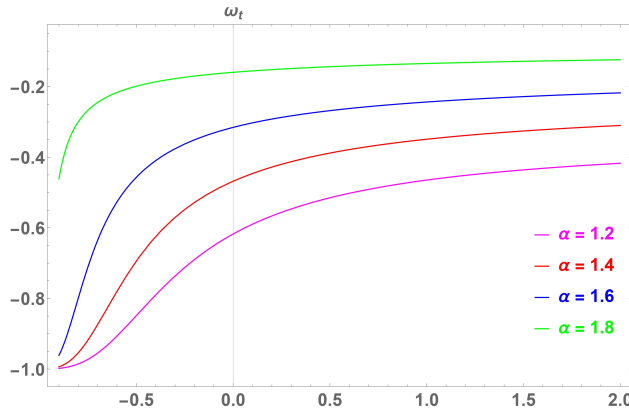


Figure 11: Plot of  $\omega_t$  against redshift  $z$  for  $\alpha = 1.2, 1.4, 1.6$  and  $1.8$ ; here  $c = 0.01$ .

We notice the following:

- In Figure 10a and Figure 10b, we perceive that the kinetic energy,  $X_t$ , and the exponential function,  $V_t(\varphi)$ , of the Tachyon field in fractional holographic reconstruction, decays to asymptotically approach  $X_t \rightarrow 0$ , and  $V_t(\varphi) \rightarrow 0$ , respectively, as the redshift  $z$  decreases in far-future limit  $z \rightarrow -1$ .

With detail:

- For larger values of  $\alpha$  (e.g.,  $\alpha = 1.8$  and  $1.6$ ),  $X_t$  shows a highly dynamic (or faster) evolution, whereas the evolution is less dynamic (or slower) for smaller values of  $\alpha$  (e.g.,  $\alpha = 1.4$  and  $1.2$ ) in the redshift region  $-1 \leq z \leq 2$ .
- On the other hand, in Figure 10b, we observe that for larger values of  $\alpha$  (e.g.,  $\alpha = 1.8$  and  $1.6$ ), the potential evolution is less dynamical (or slower) and in contrast the evolution for smaller values of  $\alpha$  (e.g.,  $\alpha = 1.2$  and  $1.4$ ), is highly dynamic in the redshift region  $-1 < z \leq 1.8$ .
- In Figure 11, we plotted for the EoS parameter,  $\omega_t$ , of the fractional holographic reconstructed Tachyon model. We can retrieve that a suitable evolution of  $\omega_t \rightarrow -1$  is possible to identify as fractional features start to dominate because it represents a scenario where the Tachyon scalar field behaves similarly to the  $\Lambda$ CDM model during dark energy dominated phase.

We discern a similar behaviour for the EoS parameter for quintessence (see Figure 2), K-essence (see Figure 4) and Yang-Mills condensate (see Figure 7b) in the far-future limit.

Briefly, Figure 10a suggests that a higher value of  $\alpha$  may not provide a suitable scenario because it does not ensure a slow-evolving field, not suggesting a nearly constant dark energy behaviour. On the other hand, in Figure 10b, a higher value of  $\alpha$  is preferable (over smaller values) because it induces a suitable situation for the potential in the redshift region  $-1 < z \leq 1.8$ .

## 4 Discussion and Outlook

The generic purpose embraced in this paper was to contribute towards a research programme that promotes an interplay between the Holographic Principle and particular features from Fractional Calculus [de Oliveira and Tenreiro Machado, 2014, Miller and Ross, 1993, Grigoletto and Oliveira, 2013]. This setting is Fractional Holographic Dark Energy (FHDE) and was introduced in [Trivedi et al., 2024], supported with concrete examples of applications.

The concrete focus we took and that guided our work throughout was to make progress, investigating whether FHDE can be a realistic and valued pretender to explain the late-time accelerated expansion of the universe. To be more precise, we methodically selected and appraised suitable field frameworks, such that they could satisfactorily encompass the alluring dynamic properties of FHDE as explained in [Trivedi et al., 2024].

In more detail, we have considered the late time evolution of the Universe within a twofold strategy. On the one hand, we employed particular effective field configurations, importing features from known settings involving spin-0 and spin-1 features. On the other hand, we used particular fractional calculus elements [Ortigueira, 2011, Ortigueira et al., 2017, Ortigueira and Trujillo, 2012, Ortigueira and Bengochea, 2023, Valério and Ortigueira, 2023, Bengochea and Ortigueira, 2023, Ortigueira, 2024] that have been considered in several gravitational scenarios [García-Aspeitia et al., 2022, Micolta-Riascos et al., 2023, Leon Torres et al., 2023, Calcagni, 2010].

A twofold query was discussed. On the one hand, can FHDE [Trivedi et al., 2024] indeed be perceived as a promising aspirant with the assistance of suitable field frameworks? On the other hand, can a suitable correspondence between those frameworks be established with the FHDE model, unveiling scenarios for dynamic dark energy from a new angle? Assuming the Hubble horizon as the IR cut-off, we investigated the following effective field configurations: (i) Quintessence, (ii) Kinetic Quintessence (K-essence), (iii) Dilaton, (iv) Yang-Mills condensate, (v) Dirac-Born-Infeld-essence (DBI-essence), and (vi) Tachyon scalar field. To prospect whether such correspondence for the above-mentioned (i)-(vi) configurations can be found within the FHDE scenario, we reconstructed two quantities: (a) kinetic energy,  $X_i$ , and (b) potential,  $V_i(\varphi)$ , with varying redshift, where  $i$  is a dummy index representing the effective field models. We then produced suitable plots of these quantities and the EoS parameter for various values of the fractional parameter  $\alpha$  such as  $\alpha = 1.2, 1.4, 1.6$  and  $1.8$ .

Our results, concerning the reconstruction of FHDE features by means of selected field configurations, can be assembled as follows:

- Let us firstly review the behaviour of  $X_i$ :
  - Among all the field configurations we used, a common feature is remarked for Quintessence (Figure 1a), K-essence (Figure 3a), DBI-essence (Figure 8a), and Tachyon scalar field (Figure 10a) which establishes that over the redshift region  $-1 < z \leq 2$ , an adequate course for  $X_i$  is appropriately described by a *smaller* value of the fractional parameter, for example,  $\alpha = 1.2$ . Concretely, it bears a less dynamic or slowly evolving behaviour as the redshift  $z$  decreases. This behaviour for smaller  $\alpha$  values strongly suggest that field configuration exhibits slow variation, associated with the field energy asymptotically approaching stabilisation with the decreasing of the field potential  $V_i(\varphi)$  (for all values of  $\alpha$ ) as  $z \rightarrow -1$  during dark energy domination.



- In the case of Dilaton (Figure 5a), the *larger* values of  $\alpha$ , like  $\alpha = 1.8$  and  $1.6$ , show a less dynamic behaviour as the redshift decreases below  $z < 1.4$ , making larger values of  $\alpha$  more suitable in the redshift region  $-1 < z \leq 1.5$ .

This distinguishes Dilaton as an exception compared to other effective field configurations, wherein a smaller value of  $\alpha$  typically indicates suitable behaviour as the Universe transitions to dark energy domination in the asymptotic future limit  $z \rightarrow -1$ .

- Moreover, for gauge field configuration, i.e., YMC, we notice that the electric field component,  $E^2$ , represents a scenario where the evolution described by *smaller* values of  $\alpha$  is more suitable compared to evolution described by larger values of  $\alpha$  as redshift  $z$  decreases.
- Regarding the pattern of  $V_i(\varphi)$  and the coupling function  $f_{kq}(\varphi)$ :
  - For Quintessence (Figure 1b), DBI-essence (Figure 8b), and Tachyon (Figure 10b) and the coupling function  $f_{kq}(\varphi)$  of K-essence (Figure 3b), they exhibit a common behaviour.

In these models, the potential decreases less dynamically for *larger* values of  $\alpha$ , such as  $\alpha = 1.8$  and  $\alpha = 1.6$ , as the redshift  $z$  decreases below certain thresholds.

Specifically, for Quintessence, this less dynamic decrease occurs as the redshift decreases below  $z < 0.55$  (Figure 1b), for DBI-essence below  $z < 0.99$  (Figure 8b), and for Tachyon below  $z < 1.8$  (Figure 10b).

Conversely, the coupling function  $f_{kq}(\varphi)$  for K-essence demonstrates a less dynamic evolution for  $\alpha = 1.8$  across the entire redshift range  $-1 < z \leq 2$ , without exhibiting a switch in  $\alpha$  value, unlike the observations in Quintessence, DBI-essence, and Tachyon.

- For Dilaton (Figure 5b), it is observed that the potential  $\beta \exp(\lambda\varphi)X_d$  exhibits a less dynamic behaviour for *smaller* values of  $\alpha$ , such as  $\alpha = 1.2$  and  $\alpha = 1.4$ , in contrast to Quintessence, DBI-essence, Tachyon, and K-essence. The potential,  $\beta \exp(\lambda\varphi)X_d$ , asymptotically approaches  $\Lambda$ CDM behaviour in the far-future limit  $z \rightarrow -1$ .
- Regarding the EoS parameter, the following should be mentioned:
  - In the case of Quintessence (Figure 2), K-essence (Figure 4), Dilaton (Figure 6), YMC (Figure 7b), and Tachyon (Figure 11), it can be noticed that for *small* values of  $\alpha$ , like  $\alpha = 1.2$  and  $1.4$ , the EoS parameter for these effective field configurations asymptotically approaches  $\Lambda$ CDM behaviour:  $\omega_i(z) \rightarrow -1$ ; in the far-future limit  $z \rightarrow -1$ .
  - In particular, for  $\alpha = 1.2$ , the EoS parameter takes a value at  $z = 0$ , which is in close agreement with the recent constraint on the EoS parameter by DESI Collaboration [Collaboration et al., 2024a,b,c].
  - However, for DBI-essence (Figure 9), the EoS parameter at  $z = 0$  deviates slightly, being *larger* than observed in other effective field configurations.

In closing, we successfully reconstructed selected field (kinetic and potential) features within the fractional holographic framework introduced in [Trivedi et al., 2024]. Our analysis demonstrated that fractional modifications help to alleviate quantum instabilities by ensuring that the EoS parameter remains above the phantom divide i.e.,  $\omega(z) < -1$ . We found that smaller values of the fractional parameter  $\alpha$  lead to a suitable evolution that asymptotically approaches a  $\Lambda$ CDM behaviour in the far-future limit  $z \rightarrow -1$ . In particular, for string theory-inspired field configurations, such as Dilaton, DBI-essence, and the Tachyon field, we found that their EoS parameter exhibits a suitable late-time cosmic acceleration, especially for small values of  $\alpha$ , prompting that fractional modifications can provide an effective description of dark energy in such frameworks. However, since string theory lacks direct experimental verification, the exact nature of dark energy within these models remains an open question. On the other hand, Quintessence, K-essence, and Yang-Mills condensates (YMC) emerge as strong alternatives, especially when employing fractional modifications. These field configurations provide a viable framework for exploring dark energy while remaining testable against observational constraints such as CMB anisotropies, BAOs, and Supernova data.

Thus, upon the progress displayed in [Trivedi et al., 2024] and herewith this paper, we place confidence in the FHDE scenario and list a few subsequent lines that we aim to pick up as future work.

On the one hand, if fractional calculus bears significance in at least dark energy physics, then it must be "observed". How can we design a test? We are pondering about a behaviour emerging for late-time data that only  $\alpha \neq 2$  and no other feature can bring.

One of the possibilities is to explore the impact of FHDE on the Integrated Sachs-Wolfe (ISW) effect, given its sensitivity to evolving gravitational potentials in the late universe. A fractional calculus-inspired modification of dark energy (e.g., FHDE) might imprint detectable deviations in Cosmic Microwave Background-Large Scale Structure (CMB-LSS) correlations and provide an alternative observational probe beyond the constraints of SNe Ia (see [Ade et al., 2016, Giannantonio et al., 2012] and [Stözlner et al., 2018] for further commentary on the ISW effect).

Furthermore, future work could also refine observational constraints to better distinguish these effective field configurations reconstructed with fractional holographic considerations.

Additionally, the dynamic stability of fractional holographic models in a non-flat Universe, i.e.,  $k \neq 0$ , plus the interaction between dark matter-dark energy, exploring connections with modified gravity frameworks, and employing more evolved cut-off(s) such as Granda-Oliveros and Nojiri-Odintsov cut-off, all these warrant further investigation within the paradigm of the FHDE scenario.

Future work could also be done to investigate the emergence of asymptotic future singularities such as "big rip" at the classical level [Caldwell, 2002].

## Acknowledgements

PM acknowledges the FCT grant UID-B-MAT/00212/2020 at CMA-UBI plus the COST Actions CA23130 (Bridging high and low energies in search of quantum gravity (BridgeQG)) and CA23115 (Relativistic Quantum Information (RQI)).

## A Appendix

In [Trivedi et al., 2024], we describe the fractional density parameter  $\Omega_{\text{de}}$  using a differential equation which can be written in the most general form as,

$$(1+z) \frac{d\Omega_{\text{de}}}{dz} = 3 \left( \frac{\alpha-2}{3\alpha-2} \right) \left( \frac{(3\alpha-2)(1-\Omega_{\text{de}}) + 2\alpha\gamma}{2\alpha - \Omega_{\text{de}}(3\alpha-2)} - \gamma \right) \Omega_{\text{de}}. \quad (54)$$

Here  $\gamma$  represents the coupling constant. However, within the scope of this work, we stick with a non-interacting scenario where  $\gamma = 0$ . The Eq. (54) becomes,

$$(1+z) \frac{d\Omega_{\text{de}}}{dz} = \frac{3(\alpha-2)(1-\Omega_{\text{de}})}{2\alpha - \Omega_{\text{de}}(3\alpha-2)} \Omega_{\text{de}}. \quad (55)$$

Upon solving this differential equation, we obtain the following expression for  $\Omega_{\text{de}}$  as,

$$\Omega_{\text{de}} = \Omega_0 \left( \frac{1-\Omega_{\text{de}}}{1-\Omega_0} \right)^{\frac{2-\alpha}{2\alpha}} (1+z)^{\frac{3(\alpha-2)}{2\alpha}}. \quad (56)$$

For the sake of completeness, an implicit equation of fractional density parameter for dark matter can be obtained as a function of redshift by using the Friedmann equation:  $\Omega_{\text{dm}} = 1 - \Omega_{\text{de}}$ . We obtain,

$$\Omega_{\text{dm}} = 1 - \Omega_0 \left( \frac{1-\Omega_{\text{de}}}{1-\Omega_0} \right)^{\frac{2-\alpha}{2\alpha}} (1+z)^{\frac{3(\alpha-2)}{2\alpha}}. \quad (57)$$

Now we proceed to obtain an implicit expression for the Hubble parameter  $H(z)$  as a function of the redshift parameter by plugging in  $\Omega_{\text{de}} = c^2 H^{\frac{\alpha-2}{\alpha}}$  in Eq. (55). We obtain,

$$H(z) = H_0 \left[ \frac{c^2 - H_0^{\frac{2-\alpha}{\alpha}}}{c^2 - H^{\frac{2-\alpha}{\alpha}}} \right]^{\frac{\alpha}{3\alpha-2}} (1+z)^{\frac{3\alpha}{(3\alpha-2)}}. \quad (58)$$

These expressions play a pivotal role in obtaining the desired plots for the dynamic-dark-energy candidates in correspondence with the FHDE model. We have set the constants  $H_0 = 70 \text{ km} \cdot \text{Mpc}^{-1} \cdot \text{s}^{-1}$ ,  $\Omega_0 = 0.69$  and  $c = 0.01$ .

## References

- Oem Trivedi, Ayush Bidlan, and Paulo Moniz. Fractional holographic dark energy. *Phys. Lett. B*, 858:139074, 2024. doi: 10.1016/j.physletb.2024.139074.
- Adam G. Riess, Alexei V. Filippenko, Peter Challis, Alejandro Clocchiatti, Alan Diercks, Peter M. Garnavich, Ron L. Gilliland, Craig J. Hogan, Saurabh Jha, Robert P. Kirshner, B. Leibundgut, M. M. Phillips, David Reiss, Brian P. Schmidt, Robert A. Schommer, R. Chris Smith, J. Spyromilio, Christopher Stubbs, Nicholas B. Suntzeff, and John Tonry. Observational evidence from supernovae for an accelerating universe and a cosmological constant. *The Astronomical Journal*, 116(3):1009–1038, September 1998. ISSN 0004-6256. doi: 10.1086/300499. URL <http://dx.doi.org/10.1086/300499>.
- S. Perlmutter, G. Aldering, G. Goldhaber, R. A. Knop, P. Nugent, P. G. Castro, S. Deustua, S. Fabbro, A. Goobar, D. E. Groom, I. M. Hook, A. G. Kim, M. Y. Kim, J. C. Lee, N. J. Nunes, R. Pain, C. R. Pennypacker, R. Quimby, C. Lidman, R. S. Ellis, M. Irwin, R. G. McMahon, P. Ruiz-Lapuente, N. Walton, B. Schaefer, B. J. Boyle, A. V. Filippenko, T. Matheson, A. S. Fruchter, N. Panagia, H. J. M. Newberg, W. J. Couch, and The Supernova Cosmology Project. Measurements of  $\Omega$  and  $\Omega$  from 42 high-redshift supernovae. *The Astrophysical Journal*, 517(2):565–586, June 1999. ISSN 1538-4357. doi: 10.1086/307221. URL <http://dx.doi.org/10.1086/307221>.
- P. Astier, J. Guy, N. Regnault, R. Pain, E. Aubourg, D. Balam, S. Basa, R. G. Carlberg, S. Fabbro, D. Fouchez, I. M. Hook, D. A. Howell, H. Lafoux, J. D. Neill, N. Palanque-Delabrouille, K. Perrett, C. J. Pritchett, J. Rich, M. Sullivan, R. Taitel, G. Aldering, P. Antilogus, V. Arsenijevic, C. Balland, S. Baumont, J. Bronder, H. Courtois, R. S. Ellis, M. Filiol, A. C. Gonçalves, A. Goobar, D. Guide, D. Hardin, V. Lusser, C. Lidman, R. McMahon, M. Mouchet, A. Mourao, S. Perlmutter, P. Ripoche, C. Tao, and N. Walton. The supernova legacy survey: measurement of  $\omega_m$ ,  $\omega_\Lambda$  and  $w$  from the first year data set. *Astronomy & Astrophysics*, 447(1):31–48, January 2006. ISSN 1432-0746. doi: 10.1051/0004-6361:20054185. URL <http://dx.doi.org/10.1051/0004-6361:20054185>.
- Adam G. Riess, Louis-Gregory Strolger, John Tonry, Stefano Casertano, Henry C. Ferguson, Bahram Mobasher, Peter Challis, Alexei V. Filippenko, Saurabh Jha, Weidong Li, Ryan Chornock, Robert P. Kirshner, Bruno Leibundgut, Mark Dickinson, Mario Livio, Mauro Giavalisco, Charles C. Steidel, Txitxo Benitez, and Zlatan Tsvetanov. Type ia supernova discoveries at  $z > 1$  from the hubble space telescope: Evidence for past deceleration and constraints on dark energy evolution. *The Astrophysical Journal*, 607(2):665–687, June 2004. ISSN 1538-4357. doi: 10.1086/383612. URL <http://dx.doi.org/10.1086/383612>.
- Adam G. Riess, Louis-Gregory Strolger, Stefano Casertano, Henry C. Ferguson, Bahram Mobasher, Ben Gold, Peter J. Challis, Alexei V. Filippenko, Saurabh Jha, Weidong Li, John Tonry, Ryan Foley, Robert P. Kirshner, Mark Dickinson, Emily MacDonald, Daniel Eisenstein, Mario Livio, Josh Younger, Chun Xu, Tomas Dahlen, and Daniel Stern. New hubble space telescopediscoveries of type ia supernovae at  $z > 1$ : Narrowing constraints on the early behavior of dark energy. *The Astrophysical Journal*, 659(1):98–121, April 2007. ISSN 1538-4357. doi: 10.1086/510378. URL <http://dx.doi.org/10.1086/510378>.
- W. M. Wood-Vasey, G. Miknaitis, C. W. Stubbs, S. Jha, A. G. Riess, P. M. Garnavich, R. P. Kirshner, C. Aguilera, A. C. Becker, J. W. Blackman, S. Blondin, P. Challis, A. Clocchiatti, A. Conley, R. Covarrubias, T. M. Davis, A. V. Filippenko, R. J. Foley, A. Garg, M. Hicken, K. Krisciunas, B. Leibundgut, W. Li, T. Matheson, A. Miceli, G. Narayan, G. Pignata, J. L. Prieto, A. Rest, M. E. Salvo, B. P. Schmidt, R. C. Smith, J. Sollerman, J. Spyromilio, J. L. Tonry, N. B. Suntzeff, and A. Zenteno. Observational constraints on the nature of dark energy: First cosmological results from the essence supernova survey. *The Astrophysical Journal*, 666(2):694–715, September 2007. ISSN 1538-4357. doi: 10.1086/518642. URL <http://dx.doi.org/10.1086/518642>.
- T. M. Davis, E. Mortsell, J. Sollerman, A. C. Becker, S. Blondin, P. Challis, A. Clocchiatti, A. V. Filippenko, R. J. Foley, P. M. Garnavich, S. Jha, K. Krisciunas, R. P. Kirshner, B. Leibundgut, W. Li, T. Matheson, G. Miknaitis, G. Pignata, A. Rest, A. G. Riess, B. P. Schmidt, R. C. Smith, J. Spyromilio, C. W. Stubbs, N. B. Suntzeff, J. L. Tonry, W. M. Wood-Vasey, and A. Zenteno. Scrutinizing exotic cosmological models using essence supernova data combined with other cosmological probes. *The Astrophysical Journal*, 666(2):716–725, September 2007. ISSN 1538-4357. doi: 10.1086/519988. URL <http://dx.doi.org/10.1086/519988>.
- M. Kowalski, D. Rubin, G. Aldering, R. J. Agostinho, A. Amadon, R. Amanullah, C. Balland, K. Barbary, G. Blanc, P. J. Challis, A. Conley, N. V. Connolly, R. Covarrubias, K. S. Dawson, S. E. Deustua, R. Ellis, S. Fabbro, V. Fadeyev, X. Fan, B. Farris, G. Folatelli, B. L. Frye, G. Garavini, E. L. Gates, L. Germany, G. Goldhaber, B. Goldman, A. Goobar, D. E. Groom, J. Haissinski, D. Hardin, I. Hook, S. Kent, A. G. Kim, R. A. Knop, C. Lidman, E. V. Linder, J. Mendez, J. Meyers, G. J. Miller, M. Moniez, A. M. Mourão, H. Newberg, S. Nobili, P. E. Nugent, R. Pain, O. Perdureau, S. Perlmutter, M. M. Phillips, V. Prasad, R. Quimby, N. Regnault, J. Rich, E. P. Rubenstein, P. Ruiz-Lapuente, F. D. Santos, B. E. Schaefer, R. A. Schommer, R. C. Smith, A. M. Soderberg, A. L. Spadafora, L.-G. Strolger, M. Strovink, N. B. Suntzeff, N. Suzuki, R. C. Thomas, N. A. Walton, L. Wang, W. M. Wood-Vasey, and J. L. Yun. Improved cosmological constraints from new, old, and combined supernova data

- sets. *The Astrophysical Journal*, 686(2):749–778, October 2008. ISSN 1538-4357. doi: 10.1086/589937. URL <http://dx.doi.org/10.1086/589937>.
- D. N. Spergel, L. Verde, H. V. Peiris, E. Komatsu, M. R. Nolta, C. L. Bennett, M. Halpern, G. Hinshaw, N. Jarosik, A. Kogut, M. Limon, S. S. Meyer, L. Page, G. S. Tucker, J. L. Weiland, E. Wollack, and E. L. Wright. First-year wilkinson microwave anisotropy probe ( wmap ) observations: Determination of cosmological parameters. *The Astrophysical Journal Supplement Series*, 148(1):175–194, September 2003. ISSN 1538-4365. doi: 10.1086/377226. URL <http://dx.doi.org/10.1086/377226>.
- D. N. Spergel, R. Bean, O. Dore, M. R. Nolta, C. L. Bennett, J. Dunkley, G. Hinshaw, N. Jarosik, E. Komatsu, L. Page, H. V. Peiris, L. Verde, M. Halpern, R. S. Hill, A. Kogut, M. Limon, S. S. Meyer, N. Odegard, G. S. Tucker, J. L. Weiland, E. Wollack, and E. L. Wright. Three-year wilkinson microwave anisotropy probe(wmap) observations: Implications for cosmology. *The Astrophysical Journal Supplement Series*, 170(2):377–408, June 2007. ISSN 1538-4365. doi: 10.1086/513700. URL <http://dx.doi.org/10.1086/513700>.
- E. Komatsu, J. Dunkley, M. R. Nolta, C. L. Bennett, B. Gold, G. Hinshaw, N. Jarosik, D. Larson, M. Limon, L. Page, D. N. Spergel, M. Halpern, R. S. Hill, A. Kogut, S. S. Meyer, G. S. Tucker, J. L. Weiland, E. Wollack, and E. L. Wright. Five-year wilkinson microwave anisotropy probe observations: Cosmological interpretation. *The Astrophysical Journal Supplement Series*, 180(2):330–376, February 2009. ISSN 1538-4365. doi: 10.1088/0067-0049/180/2/330. URL <http://dx.doi.org/10.1088/0067-0049/180/2/330>.
- E. Komatsu, K. M. Smith, J. Dunkley, C. L. Bennett, B. Gold, G. Hinshaw, N. Jarosik, D. Larson, M. R. Nolta, L. Page, D. N. Spergel, M. Halpern, R. S. Hill, A. Kogut, M. Limon, S. S. Meyer, N. Odegard, G. S. Tucker, J. L. Weiland, E. Wollack, and E. L. Wright. Seven-year wilkinson microwave anisotropy probe(wmap) observations: Cosmological interpretation. *The Astrophysical Journal Supplement Series*, 192(2):18, January 2011. ISSN 1538-4365. doi: 10.1088/0067-0049/192/2/18. URL <http://dx.doi.org/10.1088/0067-0049/192/2/18>.
- Daniel J. Eisenstein, Idit Zehavi, David W. Hogg, Roman Scoccimarro, Michael R. Blanton, Robert C. Nichol, Ryan Scranton, Hee-Jong Seo, Max Tegmark, Zheng Zheng, Scott F. Anderson, Jim Annis, Neta Bahcall, Jon Brinkmann, Scott Burles, Francisco J. Castander, Andrew Connolly, Istvan Csabai, Mamoru Doi, Masataka Fukugita, Joshua A. Frieman, Karl Glazebrook, James E. Gunn, John S. Hendry, Gregory Hennessy, Zeljko Ivezić, Stephen Kent, Gillian R. Knapp, Huan Lin, Yeong-Shang Loh, Robert H. Lupton, Bruce Margon, Timothy A. McKay, Avery Meiksin, Jeffery A. Munn, Adrian Pope, Michael W. Richmond, David Schlegel, Donald P. Schneider, Kazuhiro Shimasaku, Christopher Stoughton, Michael A. Strauss, Mark SubbaRao, Alexander S. Szalay, Istvan Szapudi, Douglas L. Tucker, Brian Yanny, and Donald G. York. Detection of the baryon acoustic peak in the large-scale correlation function of sdss luminous red galaxies. *The Astrophysical Journal*, 633(2):560–574, November 2005. ISSN 1538-4357. doi: 10.1086/466512. URL <http://dx.doi.org/10.1086/466512>.
- Will J. Percival, Shaun Cole, Daniel J. Eisenstein, Robert C. Nichol, John A. Peacock, Adrian C. Pope, and Alexander S. Szalay. Measuring the baryon acoustic oscillation scale using the sloan digital sky survey and 2df galaxy redshift survey: Measuring the bao scale. *Monthly Notices of the Royal Astronomical Society*, 381(3):1053–1066, September 2007. ISSN 1365-2966. doi: 10.1111/j.1365-2966.2007.12268.x. URL <http://dx.doi.org/10.1111/j.1365-2966.2007.12268.x>.
- Will J. Percival, Beth A. Reid, Daniel J. Eisenstein, Neta A. Bahcall, Tamas Budavari, Joshua A. Frieman, Masataka Fukugita, James E. Gunn, Željko Ivezić, Gillian R. Knapp, Richard G. Kron, Jon Loveday, Robert H. Lupton, Timothy A. McKay, Avery Meiksin, Robert C. Nichol, Adrian C. Pope, David J. Schlegel, Donald P. Schneider, David N. Spergel, Chris Stoughton, Michael A. Strauss, Alexander S. Szalay, Max Tegmark, Michael S. Vogeley, David H. Weinberg, Donald G. York, and Idit Zehavi. Baryon acoustic oscillations in the sloan digital sky survey data release 7 galaxy sample. *Monthly Notices of the Royal Astronomical Society*, 401(4):2148–2168, February 2010. ISSN 1365-2966. doi: 10.1111/j.1365-2966.2009.15812.x. URL <http://dx.doi.org/10.1111/j.1365-2966.2009.15812.x>.
- Steven Weinberg. The Cosmological Constant Problem. *Rev. Mod. Phys.*, 61:1–23, 1989. doi: 10.1103/RevModPhys.61.1.
- T. Padmanabhan. Cosmological constant: The Weight of the vacuum. *Phys. Rept.*, 380:235–320, 2003. doi: 10.1016/S0370-1573(03)00120-0.
- Michael S. Turner. The case for  $\Lambda$ cdm, 1997. URL <https://arxiv.org/abs/astro-ph/9703161>.
- G. R. Blumenthal, S. M. Faber, J. R. Primack, and M. J. Rees. Formation of galaxies and large-scale structure with cold dark matter. *Nature*, 311:517–525, October 1984. doi: 10.1038/311517a0.
- Leandros Perivolaropoulos and Foteini Skara. Challenges for  $\Lambda$ CDM: An update. *New Astron. Rev.*, 95:101659, 2022. doi: 10.1016/j.newar.2022.101659.

- J. J. Condon and A. M. Matthews.  $\Lambda$ CDM Cosmology for Astronomers. *Publ. Astron. Soc. Pac.*, 130(989):073001, 2018. doi: 10.1088/1538-3873/aac1b2.
- Lucas Lombriser. On the cosmological constant problem. *Phys. Lett. B*, 797:134804, 2019. doi: 10.1016/j.physletb.2019.134804.
- EDMUND J. COPELAND, M. SAMI, and SHINJI TSUJIKAWA. Dynamics of dark energy. *International Journal of Modern Physics D*, 15(11):1753–1935, November 2006. ISSN 1793-6594. doi: 10.1142/s021827180600942x. URL <http://dx.doi.org/10.1142/S021827180600942X>.
- M. O. Ribas, F. P. Devecchi, and G. M. Kremer. Fermions as sources of accelerated regimes in cosmology. *Phys. Rev. D*, 72:123502, 2005. doi: 10.1103/PhysRevD.72.123502. URL <https://link.aps.org/doi/10.1103/PhysRevD.72.123502>.
- Yi-Fu Cai and Jing Wang. Dark energy model with spinor matter and its quintom scenario. *Classical and Quantum Gravity*, 25(16):165014, 2008. doi: 10.1088/0264-9381/25/16/165014. URL <https://dx.doi.org/10.1088/0264-9381/25/16/165014>.
- Urjit A. Yajnik. Dark energy from ferromagnetic condensation of cosmic magninos, 2011. URL <https://arxiv.org/abs/1102.2562>.
- P. Tsyba, K. Yerzhanov, K. Esmakhanova, I. Kulnazarov, G. Nugmanova, and R. Myrzakulov. Reconstruction of f-essence and fermionic chaplygin gas models of dark energy, 2011. URL <https://arxiv.org/abs/1103.5918>.
- C. Armendáriz-Picón, T. Damour, and V. Mukhanov. k-inflation. *Physics Letters B*, 458(2–3):209–218, July 1999. ISSN 0370-2693. doi: 10.1016/s0370-2693(99)00603-6. URL [http://dx.doi.org/10.1016/S0370-2693\(99\)00603-6](http://dx.doi.org/10.1016/S0370-2693(99)00603-6).
- Wen Zhao and Yang Zhang. The state equation of yang–mills field dark energy models. *Classical and Quantum Gravity*, 23(10):3405–3417, April 2006a. ISSN 1361-6382. doi: 10.1088/0264-9381/23/10/011. URL <http://dx.doi.org/10.1088/0264-9381/23/10/011>.
- Tomi S. Koivisto and Nelson J. Nunes. Inflation and dark energy from three-forms. *Physical Review D*, 80(10), November 2009. ISSN 1550-2368. doi: 10.1103/physrevd.80.103509. URL <http://dx.doi.org/10.1103/PhysRevD.80.103509>.
- Patrick Das Gupta. Dark energy and chern-simons like gravity from a dynamical four-form, 2011. URL <https://arxiv.org/abs/0905.1621>.
- Shin’ichi Nojiri and Sergei D. Odintsov. DeSitter brane universe induced by phantom and quantum effects. *Phys. Lett. B*, 565:1–9, 2003a. doi: 10.1016/S0370-2693(03)00753-6.
- Shin’ichi Nojiri and Sergei D. Odintsov. Modified gravity with negative and positive powers of the curvature: Unification of the inflation and of the cosmic acceleration. *Phys. Rev. D*, 68:123512, 2003b. doi: 10.1103/PhysRevD.68.123512.
- Shin’ichi Nojiri and Sergei D. Odintsov. AdS / CFT correspondence, conformal anomaly and quantum corrected entropy bounds. *Int. J. Mod. Phys. A*, 16:3273–3290, 2001. doi: 10.1142/S0217751X01004128.
- Shin’ichi Nojiri and Sergei D. Odintsov. Quantum de Sitter cosmology and phantom matter. *Phys. Lett. B*, 562:147–152, 2003c. doi: 10.1016/S0370-2693(03)00594-X.
- Shin’ichi Nojiri and Sergei D. Odintsov. Quantum escape of sudden future singularity. *Phys. Lett. B*, 595:1–8, 2004a. doi: 10.1016/j.physletb.2004.06.060.
- Shin’ichi Nojiri and Sergei D. Odintsov. The Final state and thermodynamics of dark energy universe. *Phys. Rev. D*, 70:103522, 2004b. doi: 10.1103/PhysRevD.70.103522.
- Shin’ichi Nojiri and Sergei D. Odintsov. Unifying phantom inflation with late-time acceleration: Scalar phantom-non-phantom transition model and generalized holographic dark energy. *Gen. Rel. Grav.*, 38:1285–1304, 2006a. doi: 10.1007/s10714-006-0301-6.
- Shin’ichi Nojiri and Sergei D. Odintsov. Inhomogeneous equation of state of the universe: Phantom era, future singularity and crossing the phantom barrier. *Phys. Rev. D*, 72:023003, 2005. doi: 10.1103/PhysRevD.72.023003.
- Shin’ichi Nojiri, Sergei D. Odintsov, and Shinji Tsujikawa. Properties of singularities in (phantom) dark energy universe. *Phys. Rev. D*, 71:063004, 2005. doi: 10.1103/PhysRevD.71.063004.
- Shin’ichi Nojiri and Sergei D. Odintsov. Modified f(R) gravity consistent with realistic cosmology: From matter dominated epoch to dark energy universe. *Phys. Rev. D*, 74:086005, 2006b. doi: 10.1103/PhysRevD.74.086005.

- V. F. Cardone, A. Troisi, and S. Capozziello. Unified dark energy models: A phenomenological approach. *Physical Review D*, 69(8), April 2004. ISSN 1550-2368. doi: 10.1103/physrevd.69.083517. URL <http://dx.doi.org/10.1103/PhysRevD.69.083517>.
- Andronikos Paliathanasis and Genly Leon. Dynamics of a two scalar field cosmological model with phantom terms. *Classical and Quantum Gravity*, 38(7):075013, March 2021. ISSN 1361-6382. doi: 10.1088/1361-6382/abe2d7. URL <http://dx.doi.org/10.1088/1361-6382/abe2d7>.
- Sumit K. Garg and Chethan Krishnan. Bounds on slow roll and the de sitter swampland. *Journal of High Energy Physics*, 2019(11), November 2019. ISSN 1029-8479. doi: 10.1007/jhep11(2019)075. URL [http://dx.doi.org/10.1007/JHEP11\(2019\)075](http://dx.doi.org/10.1007/JHEP11(2019)075).
- Rafael Bravo, Gonzalo A. Palma, and Simón Riquelme. A tip for landscape riders: multi-field inflation can fulfill the swampland distance conjecture. *Journal of Cosmology and Astroparticle Physics*, 2020(02):004–004, February 2020. ISSN 1475-7516. doi: 10.1088/1475-7516/2020/02/004. URL <http://dx.doi.org/10.1088/1475-7516/2020/02/004>.
- Ana Achúcarro and Gonzalo A. Palma. The string swampland constraints require multi-field inflation. *Journal of Cosmology and Astroparticle Physics*, 2019(02):041–041, February 2019. ISSN 1475-7516. doi: 10.1088/1475-7516/2019/02/041. URL <http://dx.doi.org/10.1088/1475-7516/2019/02/041>.
- DESI Collaboration, A. G. Adame, J. Aguilar, S. Ahlen, S. Alam, D. M. Alexander, M. Alvarez, O. Alves, A. Anand, U. Andrade, E. Armengaud, S. Avila, A. Aviles, H. Awan, B. Bahr-Kalus, S. Bailey, C. Baltay, A. Bault, J. Behera, S. BenZvi, A. Bera, F. Beutler, D. Bianchi, C. Blake, R. Blum, S. Brieden, A. Brodzeller, D. Brooks, E. Buckley-Geer, E. Burtin, R. Calderon, R. Canning, A. Carnero Rosell, R. Cereskaite, J. L. Cervantes-Cota, S. Chabanier, E. Chaussidon, J. Chaves-Montero, S. Chen, X. Chen, T. Claybaugh, S. Cole, A. Cuceu, T. M. Davis, K. Dawson, A. de la Macorra, A. de Mattia, N. Deiosso, A. Dey, B. Dey, Z. Ding, P. Doel, J. Edelman, S. Eftekharzadeh, D. J. Eisenstein, A. Elliott, P. Fagrelus, K. Fanning, S. Ferraro, J. Ereza, N. Findlay, B. Flaugher, A. Font-Ribera, D. Forero-Sánchez, J. E. Forero-Romero, C. S. Frenk, C. Garcia-Quintero, E. Gaztañaga, H. Gil-Marín, S. Gontcho A Gontcho, A. X. Gonzalez-Morales, V. Gonzalez-Perez, C. Gordon, D. Green, D. Gruen, R. Gspaner, G. Gutierrez, J. Guy, B. Hadzhiyska, C. Hahn, M. M. S Hanif, H. K. Herrera-Alcantar, K. Honscheid, C. Howlett, D. Huterer, V. Iršič, M. Ishak, S. Juneau, N. G. Karaçaylı, R. Kehoe, S. Kent, D. Kirkby, A. Kremin, A. Krolewski, Y. Lai, T. W. Lan, M. Landriau, D. Lang, J. Lasker, J. M. Le Goff, L. Le Guillou, A. Leauthaud, M. E. Levi, T. S. Li, E. Linder, K. Lodha, C. Magneville, M. Manera, D. Margala, P. Martini, M. Maus, P. McDonald, L. Medina-Varela, A. Meisner, J. Mena-Fernández, R. Miquel, J. Moon, S. Moore, J. Moustakas, N. Mudur, E. Mueller, A. Muñoz-Gutiérrez, A. D. Myers, S. Nadathur, L. Napolitano, R. Neveux, J. A. Newman, N. M. Nguyen, J. Nie, G. Niz, H. E. Noriega, N. Padmanabhan, E. Paillas, N. Palanque-Delabrouille, J. Pan, S. Penmetsa, W. J. Percival, M. M. Pieri, M. Pinon, C. Poppett, A. Porredon, F. Prada, A. Pérez-Fernández, I. Pérez-Ràfols, D. Rabinowitz, A. Raichoor, C. Ramírez-Pérez, S. Ramírez-Solano, C. Ravoux, M. Rashkovetskyi, M. Rezaie, J. Rich, A. Rocher, C. Rockosi, N. A. Roe, A. Rosado-Marin, A. J. Ross, G. Rossi, R. Ruggeri, V. Ruhlmann-Kleider, L. Samushia, E. Sanchez, C. Saulder, E. F. Schlafly, D. Schlegel, M. Schubnell, H. Seo, A. Shafieloo, R. Sharples, J. Silber, A. Slosar, A. Smith, D. Sprayberry, T. Tan, G. Tarlé, P. Taylor, S. Trusov, L. A. Ureña-López, R. Vaisakh, D. Valcin, F. Valdes, M. Vargas-Magaña, L. Verde, M. Walther, B. Wang, M. S. Wang, B. A. Weaver, N. Weaverdyck, R. H. Wechsler, D. H. Weinberg, M. White, J. Yu, Y. Yu, S. Yuan, C. Yèche, E. A. Zaborowski, P. Zarrouk, H. Zhang, C. Zhao, R. Zhao, R. Zhou, T. Zhuang, and H. Zou. Desi 2024 vi: Cosmological constraints from the measurements of baryon acoustic oscillations, 2024a. URL <https://arxiv.org/abs/2404.03002>.
- K. Lodha, A. Shafieloo, R. Calderon, E. Linder, W. Sohn, J. L. Cervantes-Cota, A. de Mattia, J. García-Bellido, M. Ishak, W. Matthewson, J. Aguilar, S. Ahlen, D. Brooks, T. Claybaugh, A. de la Macorra, A. Dey, B. Dey, P. Doel, J. E. Forero-Romero, E. Gaztañaga, S. Gontcho A Gontcho, C. Howlett, S. Juneau, S. Kent, T. Kisner, A. Kremin, A. Lambert, M. Landriau, L. Le Guillou, P. Martini, A. Meisner, R. Miquel, J. Moustakas, J. A. Newman, G. Niz, N. Palanque-Delabrouille, W. J. Percival, C. Poppett, F. Prada, G. Rossi, V. Ruhlmann-Kleider, E. Sanchez, E. F. Schlafly, D. Schlegel, M. Schubnell, H. Seo, D. Sprayberry, G. Tarlé, B. A. Weaver, and H. Zou. Desi 2024: Constraints on physics-focused aspects of dark energy using desi dr1 bao data, 2024. URL <https://arxiv.org/abs/2405.13588>.
- R. Calderon, K. Lodha, A. Shafieloo, E. Linder, W. Sohn, A. de Mattia, J.L. Cervantes-Cota, R. Crittenden, T.M. Davis, M. Ishak, A.G. Kim, W. Matthewson, G. Niz, S. Park, J. Aguilar, S. Ahlen, S. Allen, D. Brooks, T. Claybaugh, A. de la Macorra, A. Dey, B. Dey, P. Doel, J.E. Forero-Romero, E. Gaztañaga, S.Gontcho A. Gontcho, K. Honscheid, C. Howlett, S. Juneau, A. Kremin, M. Landriau, L. Le Guillou, M.E. Levi, M. Manera, R. Miquel, J. Moustakas, J.A. Newman, N. Palanque-Delabrouille, W.J. Percival, C. Poppett, F. Prada, M. Rezaie, G. Rossi, V. Ruhlmann-Kleider, E. Sanchez, D. Schlegel, M. Schubnell, H. Seo, D. Sprayberry, G. Tarlé, P. Taylor, M. Vargas-Magaña, B.A. Weaver, P. Zarrouk, and H. Zou. Desi 2024: reconstructing dark energy using crossing statistics with desi dr1

- bao data. *Journal of Cosmology and Astroparticle Physics*, 2024(10):048, October 2024. ISSN 1475-7516. doi: 10.1088/1475-7516/2024/10/048. URL <http://dx.doi.org/10.1088/1475-7516/2024/10/048>.
- Miao Li. A Model of holographic dark energy. *Phys. Lett. B*, 603:1, 2004. doi: 10.1016/j.physletb.2004.10.014.
- Leonard Susskind. The World as a hologram. *J. Math. Phys.*, 36:6377–6396, 1995. doi: 10.1063/1.531249.
- Edmundo Capelas de Oliveira and José António Tenreiro Machado. A review of definitions for fractional derivatives and integral. *Mathematical Problems in Engineering*, 2014(1):238459, 2014. doi: <https://doi.org/10.1155/2014/238459>. URL <https://onlinelibrary.wiley.com/doi/abs/10.1155/2014/238459>.
- Kenneth S. Miller and Bertram Ross. An introduction to the fractional calculus and fractional differential equations. In *An Introduction to the Fractional Calculus and Fractional Differential Equations*, 1993. URL <https://api.semanticscholar.org/CorpusID:117250850>.
- Eliana Contharteze Grigoletto and Edmundo Capelas De Oliveira. Fractional versions of the fundamental theorem of calculus. *Applied Mathematics-a Journal of Chinese Universities Series B*, 2013:23–33, 2013. URL <https://api.semanticscholar.org/CorpusID:55508527>.
- Ahmad Sheykhi. Holographic scalar field models of dark energy. *Physical Review D*, 84(10), November 2011. ISSN 1550-2368. doi: 10.1103/physrevd.84.107302. URL <http://dx.doi.org/10.1103/PhysRevD.84.107302>.
- Xin Zhang. Reconstructing holographic quintessence. *Physics Letters B*, 648(1):1–7, 2007. ISSN 0370-2693. doi: <https://doi.org/10.1016/j.physletb.2007.02.069>. URL <https://www.sciencedirect.com/science/article/pii/S0370269307002663>.
- Jian-Pin Wu, Da-Zhu Ma, and Yi Ling. Quintessence reconstruction of the new agegraphic dark energy model. *Physics Letters B*, 663(3):152–159, 2008. ISSN 0370-2693. doi: <https://doi.org/10.1016/j.physletb.2008.03.071>. URL <https://www.sciencedirect.com/science/article/pii/S0370269308004048>.
- Ahmad Sheykhi. Interacting agegraphic tachyon model of dark energy. *Physics Letters B*, 682(4):329–333, 2010. ISSN 0370-2693. doi: <https://doi.org/10.1016/j.physletb.2009.11.034>. URL <https://www.sciencedirect.com/science/article/pii/S037026930901380X>.
- K. Karami and J. Fehri. New holographic scalar field models of dark energy in non-flat universe. *Physics Letters B*, 684(2):61–68, 2010. ISSN 0370-2693. doi: <https://doi.org/10.1016/j.physletb.2009.12.060>. URL <https://www.sciencedirect.com/science/article/pii/S0370269310000122>.
- Ulbosyn Ualikhanova, Aziza Altaibayeva, and Surajit Chattopadhyay. Holographic reconstruction of k-essence model with tsallis and the most generalized nojiri-odintsov version of holographic dark energy, 2024. URL <https://arxiv.org/abs/2501.04028>.
- Umesh Kumar Sharma, Mukesh Kumar, and Gunjan Varshney. Scalar field models of barrow holographic dark energy in  $f(r,t)$  gravity. *Universe*, 8(12), 2022. ISSN 2218-1997. doi: 10.3390/universe8120642. URL <https://www.mdpi.com/2218-1997/8/12/642>.
- S. Jalalzadeh, F. Rodrigues da Silva, and P. V. Moniz. Prospecting black hole thermodynamics with fractional quantum mechanics. *The European Physical Journal C*, 81(7), July 2021. ISSN 1434-6052. doi: 10.1140/epjc/s10052-021-09438-5. URL <http://dx.doi.org/10.1140/epjc/s10052-021-09438-5>.
- A Sheykhi, A Bagheri, and M.M Yazdanpanah. Interacting agegraphic quintessence dark energy in non-flat universe. *Journal of Cosmology and Astroparticle Physics*, 2010(09):017–017, September 2010. ISSN 1475-7516. doi: 10.1088/1475-7516/2010/09/017. URL <http://dx.doi.org/10.1088/1475-7516/2010/09/017>.
- L.N. Granda and A. Oliveros. Infrared cut-off proposal for the holographic density. *Physics Letters B*, 669(5):275–277, November 2008. ISSN 0370-2693. doi: 10.1016/j.physletb.2008.10.017. URL <http://dx.doi.org/10.1016/j.physletb.2008.10.017>.
- Hyeong-Chan Kim, Jae-Weon Lee, and Jungjai Lee. Causality problem in a holographic-dark-energy model. *EPL (Europhysics Letters)*, 102(2):29001, April 2013. ISSN 1286-4854. doi: 10.1209/0295-5075/102/29001. URL <http://dx.doi.org/10.1209/0295-5075/102/29001>.
- Shin’ichi Nojiri and S. D. Odintsov. Covariant Generalized Holographic Dark Energy and Accelerating Universe. *Eur. Phys. J. C*, 77(8):528, 2017. doi: 10.1140/epjc/s10052-017-5097-x.
- Shin’ichi Nojiri, Sergei D. Odintsov, and Emmanuel N. Saridakis. Holographic bounce. *Nuclear Physics B*, 949: 114790, December 2019. ISSN 0550-3213. doi: 10.1016/j.nuclphysb.2019.114790. URL <http://dx.doi.org/10.1016/j.nuclphysb.2019.114790>.
- Yun Soo Myung. Instability of holographic dark energy models. *Phys. Lett. B*, 652:223–227, 2007. doi: 10.1016/j.physletb.2007.07.033.

- P. J. Steinhardt. A quintessential introduction to dark energy. *Phil. Trans. Roy. Soc. Lond. A*, 361:2497–2513, 2003. doi: 10.1098/rsta.2003.1290.
- Shinji Tsujikawa. Quintessence: A Review. *Class. Quant. Grav.*, 30:214003, 2013. doi: 10.1088/0264-9381/30/21/214003.
- Ivaylo Zlatev, Li-Min Wang, and Paul J. Steinhardt. Quintessence, cosmic coincidence, and the cosmological constant. *Phys. Rev. Lett.*, 82:896–899, 1999. doi: 10.1103/PhysRevLett.82.896.
- Roland de Putter and Eric V. Linder. Kinetic k-essence and quintessence. *Astroparticle Physics*, 28(3):263–272, November 2007. ISSN 0927-6505. doi: 10.1016/j.astropartphys.2007.05.011. URL <http://dx.doi.org/10.1016/j.astropartphys.2007.05.011>.
- E. J. Copeland, M. Sami, and S. Tsujikawa. Dynamics of dark energy. *Int. J. Mod. Phys. D*, 15:1753–1936, 2006. doi: 10.1142/S021827180600942X.
- Federico Piazza and Shinji Tsujikawa. Dilatonic ghost condensate as dark energy. *Journal of Cosmology and Astroparticle Physics*, 2004(07):004–004, July 2004. ISSN 1475-7516. doi: 10.1088/1475-7516/2004/07/004. URL <http://dx.doi.org/10.1088/1475-7516/2004/07/004>.
- Sean M. Carroll, Mark Hoffman, and Mark Trodden. Can the dark energy equation-of-state parameter be less than  $-1$ . *Physical Review D*, 68(2), July 2003. ISSN 1089-4918. doi: 10.1103/PhysRevD.68.023509. URL <http://dx.doi.org/10.1103/PhysRevD.68.023509>.
- W. Zhao, Y. Zhang, and M. L. Tong. Quantum yang-mills condensate dark energy models, 2009. URL <https://arxiv.org/abs/0909.3874>.
- Stephen L. Adler. Effective-action approach to mean-field non-abelian statics, and a model for bag formation. *Phys. Rev. D*, 23:2905–2915, 1981. doi: 10.1103/PhysRevD.23.2905. URL <https://link.aps.org/doi/10.1103/PhysRevD.23.2905>.
- Wen Zhao and Yang Zhang. Coincidence problem in ym field dark energy model. *Physics Letters B*, 640(3):69–73, September 2006b. ISSN 0370-2693. doi: 10.1016/j.physletb.2006.07.052. URL <http://dx.doi.org/10.1016/j.physletb.2006.07.052>.
- P V Moniz and J M Mourao. Homogeneous and isotropic closed cosmologies with a gauge sector. *Classical and Quantum Gravity*, 8(10):1815, 1991. doi: 10.1088/0264-9381/8/10/008. URL <https://dx.doi.org/10.1088/0264-9381/8/10/008>.
- P V Moniz, J M Mourao, and P M Sa. The dynamics of a flat friedmann-robertson-walker inflationary model in the presence of gauge fields. *Classical and Quantum Gravity*, 10(3):517, 1993. doi: 10.1088/0264-9381/10/3/012. URL <https://dx.doi.org/10.1088/0264-9381/10/3/012>.
- WEN ZHAO and DONGHUI XU. Evolution of the magnetic component in yang–mills condensate dark energy models. *International Journal of Modern Physics D*, 16(11):1735–1744, November 2007. ISSN 1793-6594. doi: 10.1142/s0218271807011048. URL <http://dx.doi.org/10.1142/S0218271807011048>.
- Changrim Ahn, Chanju Kim, and Eric V. Linder. Dark energy properties in dbi theory. *Physical Review D*, 80(12), December 2009. ISSN 1550-2368. doi: 10.1103/PhysRevD.80.123016. URL <http://dx.doi.org/10.1103/PhysRevD.80.123016>.
- Eva Silverstein and David Tong. Scalar speed limits and cosmology: Acceleration from d-celeration. *Phys. Rev. D*, 70:103505, 2004. doi: 10.1103/PhysRevD.70.103505. URL <https://link.aps.org/doi/10.1103/PhysRevD.70.103505>.
- Anupam Mazumdar, Sudhakar Panda, and Abdel Pérez-Lorenzana. Assisted inflation via tachyon condensation. *Nuclear Physics B*, 614(1–2):101–116, October 2001. ISSN 0550-3213. doi: 10.1016/s0550-3213(01)00410-2. URL [http://dx.doi.org/10.1016/S0550-3213\(01\)00410-2](http://dx.doi.org/10.1016/S0550-3213(01)00410-2).
- Alexander Feinstein. Power-law inflation from the rolling tachyon. *Physical Review D*, 66(6), September 2002. ISSN 1089-4918. doi: 10.1103/PhysRevD.66.063511. URL <http://dx.doi.org/10.1103/PhysRevD.66.063511>.
- Yun-Song Piao, Rong-Gen Cai, Xinmin Zhang, and Yuan-Zhong Zhang. Assisted tachyonic inflation. *Physical Review D*, 66(12), December 2002. ISSN 1089-4918. doi: 10.1103/PhysRevD.66.121301. URL <http://dx.doi.org/10.1103/PhysRevD.66.121301>.
- G.W Gibbons. Cosmological evolution of the rolling tachyon. *Physics Letters B*, 537(1–2):1–4, June 2002. ISSN 0370-2693. doi: 10.1016/s0370-2693(02)01881-6. URL [http://dx.doi.org/10.1016/S0370-2693\(02\)01881-6](http://dx.doi.org/10.1016/S0370-2693(02)01881-6).
- Manuel Duarte Ortigueira. *Fractional Calculus for Scientists and Engineers*. Lecture Notes in Electrical Engineering. Springer Science & Business Media, 2011. ISBN 978-94-007-0746-7. doi: 10.1007/978-94-007-0747-4.



- Manuel Ortigueira, José Tenreiro Machado, and Juan Trujillo. Fractional derivatives and periodic functions. *International Journal of Dynamics and Control*, 5, 03 2017. doi: 10.1007/s40435-015-0215-9.
- Manuel D. Ortigueira and Juan J. Trujillo. A relation between the fractional derivative and the hilbert transform. *IFAC Proceedings Volumes*, 45(2):597–599, 2012. ISSN 1474-6670. doi: <https://doi.org/10.3182/20120215-3-AT-3016.00106>. URL <https://www.sciencedirect.com/science/article/pii/S147466701630739X>. 7th Vienna International Conference on Mathematical Modelling.
- Manuel Duarte Ortigueira and Gabriel Bengochea. On the fractional derivative duality in some transforms. *Mathematics*, 11(21), 2023. ISSN 2227-7390. doi: 10.3390/math11214464. URL <https://www.mdpi.com/2227-7390/11/21/4464>.
- Duarte Valério and Manuel D. Ortigueira. Variable-order fractional scale calculus. *Mathematics*, 11(21), 2023. ISSN 2227-7390. doi: 10.3390/math11214549. URL <https://www.mdpi.com/2227-7390/11/21/4549>.
- Gabriel Bengochea and Manuel Duarte Ortigueira. An operational approach to fractional scale-invariant linear systems. *Fractal and Fractional*, 7(7), 2023. ISSN 2504-3110. doi: 10.3390/fractalfract7070524. URL <https://www.mdpi.com/2504-3110/7/7/524>.
- Manuel D. Ortigueira. A factory of fractional derivatives. *Symmetry*, 16(7), 2024. ISSN 2073-8994. doi: 10.3390/sym16070814. URL <https://www.mdpi.com/2073-8994/16/7/814>.
- Miguel A. García-Aspeitia, Guillermo Fernandez-Anaya, A. Hernández-Almada, Genly Leon, and Juan Magaña. Cosmology under the fractional calculus approach. *Mon. Not. Roy. Astron. Soc.*, 517(4):4813–4826, 2022. doi: 10.1093/mnras/stac3006.
- Bayron Micolta-Riascos, Alfredo D. Millano, Genly Leon, Cristián Erices, and Andronikos Paliathanasis. Revisiting Fractional Cosmology. *Fractal Fract.*, 7:149, 2023. doi: 10.3390/fractalfract7020149.
- Genly Leon Torres, Miguel A. García-Aspeitia, Guillermo Fernandez-Anaya, Alberto Hernández-Almada, Juan Magaña, and Esteban González. Cosmology under the fractional calculus approach: a possible  $H_0$  tension resolution? *PoS, CORFU2022:248*, 2023. doi: 10.22323/1.436.0248.
- Gianluca Calcagni. Fractal universe and quantum gravity. *Phys. Rev. Lett.*, 104:251301, 2010. doi: 10.1103/PhysRevLett.104.251301.
- DESI Collaboration, A. G. Adame, J. Aguilar, S. Ahlen, S. Alam, D. M. Alexander, M. Alvarez, O. Alves, A. Anand, U. Andrade, E. Armengaud, S. Avila, A. Aviles, H. Awan, S. Bailey, C. Baltay, A. Bault, J. Bautista, J. Behera, S. BenZvi, F. Beutler, D. Bianchi, C. Blake, R. Blum, S. Brieden, A. Brodzeller, D. Brooks, E. Buckley-Geer, E. Burtin, R. Calderon, R. Canning, A. Carnero Rosell, R. Cereskaite, J. L. Cervantes-Cota, S. Chabanier, E. Chaussidon, J. Chaves-Montero, S. Chen, X. Chen, T. Claybaugh, S. Cole, A. Cuceu, T. M. Davis, K. Dawson, R. de la Cruz, A. de la Macorra, A. de Mattia, N. Deiosso, A. Dey, B. Dey, J. Ding, Z. Ding, P. Doel, J. Edelstein, S. Eftekharzadeh, D. J. Eisenstein, A. Elliott, P. Fagrellius, K. Fanning, S. Ferraro, J. Ereza, N. Findlay, B. Flaugher, A. Font-Ribera, D. Forero-Sánchez, J. E. Forero-Romero, C. Garcia-Quintero, E. Gaztañaga, H. Gil-Marín, S. Gontcho A Gontcho, A. X. Gonzalez-Morales, V. Gonzalez-Perez, C. Gordon, D. Green, D. Gruen, R. Gspaner, G. Gutierrez, J. Guy, B. Hadzhiyska, C. Hahn, M. M. S Hanif, H. K. Herrera-Alcantar, K. Honscheid, C. Howlett, D. Huterer, V. Iršič, M. Ishak, S. Juneau, N. G. Karaçayli, R. Kehoe, S. Kent, D. Kirkby, A. Kremin, A. Krolewski, Y. Lai, T. W. Lan, M. Landriau, D. Lang, J. Lasker, J. M. Le Goff, L. Le Guillou, A. Leauthaud, M. E. Levi, T. S. Li, E. Linder, K. Lodha, C. Magneville, M. Manera, D. Margala, P. Martini, M. Maus, P. McDonald, L. Medina-Varela, A. Meisner, J. Mena-Fernández, R. Miquel, J. Moon, S. Moore, J. Moustakas, E. Mueller, A. Muñoz-Gutiérrez, A. D. Myers, S. Nadathur, L. Napolitano, R. Neveux, J. A. Newman, N. M. Nguyen, J. Nie, G. Niz, H. E. Noriega, N. Padmanabhan, E. Paillas, N. Palanque-Delabrouille, J. Pan, S. Penmetsa, W. J. Percival, M. M. Pieri, M. Pinon, C. Poppett, A. Porredon, F. Prada, A. Pérez-Fernández, I. Pérez-Ràfols, D. Rabinowitz, A. Raichoor, C. Ramírez-Pérez, S. Ramírez-Solano, M. Rashkovetskyi, C. Ravoux, M. Rezaie, J. Rich, A. Rocher, C. Rockosi, N. A. Roe, A. Rosado-Marin, A. J. Ross, G. Rossi, R. Ruggeri, V. Ruhlmann-Kleider, L. Samushia, E. Sanchez, C. Saulder, E. F. Schlafly, D. Schlegel, M. Schubnell, H. Seo, R. Sharples, J. Silber, F. Sinigaglia, A. Slosar, A. Smith, D. Sprayberry, T. Tan, G. Tarlé, S. Trusov, R. Vaisakh, D. Valcin, F. Valdes, M. Vargas-Magaña, L. Verde, M. Walther, B. Wang, M. S. Wang, B. A. Weaver, N. Weaverdyck, R. H. Wechsler, D. H. Weinberg, M. White, J. Yu, Y. Yu, S. Yuan, C. Yèche, E. A. Zaborowski, P. Zarrouk, H. Zhang, C. Zhao, R. Zhao, R. Zhou, and H. Zou. Desi 2024 iv: Baryon acoustic oscillations from the lyman alpha forest, 2024b. URL <https://arxiv.org/abs/2404.03001>.
- DESI Collaboration, A. G. Adame, J. Aguilar, S. Ahlen, S. Alam, D. M. Alexander, M. Alvarez, O. Alves, A. Anand, U. Andrade, E. Armengaud, S. Avila, A. Aviles, H. Awan, S. Bailey, C. Baltay, A. Bault, J. Behera, S. BenZvi, F. Beutler, D. Bianchi, C. Blake, R. Blum, S. Brieden, A. Brodzeller, D. Brooks, E. Buckley-Geer, E. Burtin, R. Calderon, R. Canning, A. Carnero Rosell, R. Cereskaite, J. L. Cervantes-Cota, S. Chabanier, E. Chaussidon,

- J. Chaves-Montero, S. Chen, X. Chen, T. Claybaugh, S. Cole, A. Cuceu, T. M. Davis, K. Dawson, A. de la Macorra, A. de Mattia, N. Deiosso, A. Dey, B. Dey, Z. Ding, P. Doel, J. Edelman, S. Eftekharzadeh, D. J. Eisenstein, A. Elliott, P. Fagrelus, K. Fanning, S. Ferraro, J. Ereza, N. Findlay, B. Flaughner, A. Font-Ribera, D. Forero-Sánchez, J. E. Forero-Romero, C. Garcia-Quintero, E. Gaztañaga, H. Gil-Marín, S. Gontcho A Gontcho, A. X. Gonzalez-Morales, V. Gonzalez-Perez, C. Gordon, D. Green, D. Gruen, R. Gspaner, G. Gutierrez, J. Guy, B. Hadzhiyska, C. Hahn, M. M. S Hanif, H. K. Herrera-Alcantar, K. Honscheid, C. Howlett, D. Huterer, V. Iršič, M. Ishak, S. Juneau, N. G. Karaçaylı, R. Kehoe, S. Kent, D. Kirkby, A. Kremin, A. Krolewski, Y. Lai, T. W. Lan, M. Landriau, D. Lang, J. Lasker, J. M. Le Goff, L. Le Guillou, A. Leauthaud, M. E. Levi, T. S. Li, E. Linder, K. Lodha, C. Magneville, M. Manera, D. Margala, P. Martini, M. Maus, P. McDonald, L. Medina-Varela, A. Meisner, J. Mena-Fernández, R. Miquel, J. Moon, S. Moore, J. Moustakas, N. Mudur, E. Mueller, A. Muñoz-Gutiérrez, A. D. Myers, S. Nadathur, L. Napolitano, R. Neveux, J. A. Newman, N. M. Nguyen, J. Nie, G. Niz, H. E. Noriega, N. Padmanabhan, E. Pailas, N. Palanque-Delabrouille, J. Pan, S. Penmetsa, W. J. Percival, M. Pieri, M. Pinon, C. Poppett, A. Porredon, F. Prada, A. Pérez-Fernández, I. Pérez-Ràfols, D. Rabinowitz, A. Raichoor, C. Ramírez-Pérez, S. Ramirez-Solano, M. Rashkovetskiy, M. Rezaie, J. Rich, A. Rocher, C. Rockosi, N. A. Roe, A. Rosado-Marin, A. J. Ross, G. Rossi, R. Ruggeri, V. Ruhlmann-Kleider, L. Samushia, E. Sanchez, C. Saulder, E. F. Schlafly, D. Schlegel, M. Schubnell, H. Seo, R. Sharples, J. Silber, A. Slosar, A. Smith, D. Sprayberry, J. Swanson, T. Tan, G. Tarlé, S. Trusov, R. Vaisakh, D. Valcin, F. Valdes, M. Vargas-Magaña, L. Verde, M. Walther, B. Wang, M. S. Wang, B. A. Weaver, N. Weaverdyck, R. H. Wechsler, D. H. Weinberg, M. White, J. Yu, Y. Yu, S. Yuan, C. Yèche, E. A. Zaborowski, P. Zarrouk, H. Zhang, C. Zhao, R. Zhao, R. Zhou, and H. Zou. Desi 2024 iii: Baryon acoustic oscillations from galaxies and quasars, 2024c. URL <https://arxiv.org/abs/2404.03000>.
- P. A. R. Ade, N. Aghanim, M. Arnaud, M. Ashdown, J. Aumont, C. Baccigalupi, A. J. Banday, R. B. Barreiro, N. Bartolo, S. Basak, E. Battaner, K. Benabed, A. Benoît, A. Benoit-Lévy, J.-P. Bernard, M. Bersanelli, P. Bielewicz, J. J. Bock, A. Bonaldi, L. Bonavera, J. R. Bond, J. Borrill, F. R. Bouchet, M. Bucher, C. Burigana, R. C. Butler, E. Calabrese, J.-F. Cardoso, B. Casaponsa, A. Catalano, A. Challinor, A. Chamballu, H. C. Chiang, P. R. Christensen, S. Church, D. L. Clements, S. Colombi, L. P. L. Colombo, C. Combet, F. Couchot, A. Coulais, B. P. Crill, A. Curto, F. Cuttaia, L. Danese, R. D. Davies, R. J. Davis, P. de Bernardis, A. de Rosa, G. de Zotti, J. Delabrouille, F.-X. Désert, J. M. Diego, H. Dole, S. Donzelli, O. Doré, M. Douspis, A. Ducout, X. Dupac, G. Efstathiou, F. Elsner, T. A. Enßlin, H. K. Eriksen, J. Fergusson, R. Fernandez-Cobos, F. Finelli, O. Forni, M. Frailis, A. A. Fraisse, E. Franceschi, A. Frejsel, S. Galeotta, S. Galli, K. Ganga, R. T. Génova-Santos, M. Giard, Y. Giraud-Héraud, E. Gjerløw, J. González-Nuevo, K. M. Górski, S. Gratton, A. Gregorio, A. Gruppuso, J. E. Gudmundsson, F. K. Hansen, D. Hanson, D. L. Harrison, S. Henrot-Versillé, C. Hernández-Monteagudo, D. Herranz, S. R. Hildebrandt, E. Hivon, M. Hobson, W. A. Holmes, A. Hornstrup, W. Hovest, K. M. Huffenberger, G. Hurier, S. Ilić, A. H. Jaffe, T. R. Jaffe, W. C. Jones, M. Juvela, E. Keihänen, R. Keskitalo, T. S. Kisner, R. Kneissl, J. Knoche, M. Kunz, H. Kurki-Suonio, G. Lagache, A. Lähteenmäki, J.-M. Lamarre, M. Langer, A. Lasenby, M. Lattanzi, C. R. Lawrence, R. Leonardi, J. Lesgourgues, F. Levrier, M. Liguori, P. B. Lilje, M. Linden-Vørnle, M. López-Caniiego, P. M. Lubin, Y.-Z. Ma, J. F. Macías-Pérez, G. Maggio, D. Maino, N. Mandolesi, A. Mangilli, A. Marcos-Caballero, M. Maris, P. G. Martin, E. Martínez-González, S. Masi, S. Matarrese, P. McGehee, P. R. Meinhold, A. Melchiorri, L. Mendes, A. Mennella, M. Migliaccio, S. Mitra, M.-A. Miville-Deschênes, A. Moneti, L. Montier, G. Morgante, D. Mortlock, A. Moss, D. Munshi, J. A. Murphy, P. Naselsky, F. Nati, P. Natoli, C. B. Netterfield, H. U. Nørgaard-Nielsen, F. Novello, D. Novikov, I. Novikov, C. A. Oxborrow, F. Paci, L. Pagano, F. Pajot, D. Paoletti, F. Pasian, G. Patanchon, O. Perdereau, L. Perotto, F. Perrotta, V. Pettorino, F. Piacentini, M. Piat, E. Pierpaoli, D. Pietrobon, S. Plaszczynski, E. Pointecouteau, G. Polenta, L. Popa, G. W. Pratt, G. Prézeau, S. Prunet, J.-L. Puget, J. P. Rachen, W. T. Reach, R. Rebolo, M. Reinecke, M. Remazeilles, C. Renault, A. Renzi, I. Ristorcelli, G. Rocha, C. Rosset, M. Rossetti, G. Roudier, J. A. Rubiño-Martín, B. Rusholme, M. Sandri, D. Santos, M. Savelainen, G. Savini, B. M. Schaefer, D. Scott, M. D. Seiffert, E. P. S. Shellard, L. D. Spencer, V. Stolyarov, R. Stompor, R. Sudiwala, R. Sunyaev, D. Sutton, A.-S. Suur-Uski, J.-F. Sygnet, J. A. Tauber, L. Tenzli, L. Toffolatti, M. Tomasi, M. Tristram, M. Tucci, J. Tuovinen, L. Valenziano, J. Valiviita, F. Van Tent, P. Vielva, F. Villa, L. A. Wade, B. D. Wandelt, I. K. Wehus, D. Yvon, A. Zacchei, and A. Zonca. Planck2015 results: Xxi. the integrated sachs-wolfe effect. *Astronomy & Astrophysics*, 594:A21, September 2016. ISSN 1432-0746. doi: 10.1051/0004-6361/201525831. URL <http://dx.doi.org/10.1051/0004-6361/201525831>.
- Tommaso Giannantonio, Robert Crittenden, Robert Nichol, and Ashley J. Ross. The significance of the integrated sachs-wolfe effect revisited: The significance of the isw effect revisited. *Monthly Notices of the Royal Astronomical Society*, 426(3):2581–2599, October 2012. ISSN 0035-8711. doi: 10.1111/j.1365-2966.2012.21896.x. URL <http://dx.doi.org/10.1111/j.1365-2966.2012.21896.x>.
- Benjamin Stözlner, Alessandro Cuoco, Julien Lesgourgues, and Maciej Bilicki. Updated tomographic analysis of the integrated sachs-wolfe effect and implications for dark energy. *Physical Review D*, 97(6), March 2018. ISSN 2470-0029. doi: 10.1103/physrevd.97.063506. URL <http://dx.doi.org/10.1103/PhysRevD.97.063506>.

R.R Caldwell. A phantom menace? cosmological consequences of a dark energy component with super-negative equation of state. *Physics Letters B*, 545(1–2):23–29, October 2002. ISSN 0370-2693. doi: 10.1016/S0370-2693(02)02589-3. URL [http://dx.doi.org/10.1016/S0370-2693\(02\)02589-3](http://dx.doi.org/10.1016/S0370-2693(02)02589-3).